Cellular/Molecular

Interactive HIV-1 Tat and Morphine-Induced Synaptodendritic Injury Is Triggered through Focal Disruptions in Na^+ Influx, Mitochondrial Instability, and Ca^{2+} Overload

Sylvia Fitting,[1] Pamela E. Knapp,[2,3] Shiping Zou,[2] William D. Marks,[1] M. Scott Bowers,[1,3,4] Hamid I. Akbarali,[1] and Kurt F. Hauser[1,3]

[1]Departments of Pharmacology and Toxicology, [2]Anatomy and Neurobiology, [3]Institute for Drug and Alcohol Studies, and [4]Virginia Institute for Psychiatric and Behavioral Genetics, Department of Psychiatry, Virginia Commonwealth University, Medical College of Virginia Campus, Richmond, Virginia 23298

Synaptodendritic injury is thought to underlie HIV-associated neurocognitive disorders and contributes to exaggerated inflammation and cognitive impairment seen in opioid abusers with HIV-1. To examine events triggering combined transactivator of transcription (Tat)- and morphine-induced synaptodendritic injury systematically, striatal neuron imaging studies were conducted *in vitro*. These studies demonstrated nearly identical pathologic increases in dendritic varicosities as seen in Tat transgenic mice *in vivo*. Tat caused significant focal increases in intracellular sodium ($[Na^+]_i$) and calcium ($[Ca^{2+}]_i$) in dendrites that were accompanied by the emergence of dendritic varicosities. These effects were largely, but not entirely, attenuated by the NMDA and AMPA receptor antagonists MK-801 and CNQX, respectively. Concurrent morphine treatment accelerated Tat-induced focal varicosities, which were accompanied by localized increases in $[Ca^{2+}]_i$ and exaggerated instability in mitochondrial inner membrane potential. Importantly, morphine's effects were prevented by the μ-opioid receptor antagonist CTAP and were not observed in neurons cultured from μ-opioid receptor knock-out mice. Combined Tat- and morphine-induced initial losses in ion homeostasis and increases in $[Ca^{2+}]_i$ were attenuated by the ryanodine receptor inhibitor ryanodine, as well as pyruvate. In summary, Tat induced increases in $[Na^+]_i$, mitochondrial instability, excessive Ca^{2+} influx through glutamatergic receptors, and swelling along dendrites. Morphine, acting via μ-opioid receptors, exacerbates these excitotoxic Tat effects at the same subcellular locations by mobilizing additional $[Ca^{2+}]_i$ and by further disrupting $[Ca^{2+}]_i$ homeostasis. We hypothesize that the spatiotemporal relationship of μ-opioid and aberrant AMPA/NMDA glutamate receptor signaling is critical in defining the location and degree to which opiates exacerbate the synaptodendritic injury commonly observed in neuroAIDS.

Key words: **dendritic varicosities; HIV-1 Tat; intracellular sodium; mitochondrial hyperpolarization; opioid drug abuse; striatal medium spiny neurons**

Introduction

Dendritic injury and the resultant loss of neuronal interconnections are thought to be a substrate for the neurobehavioral deficits (Masliah et al., 1997) underlying human immunodeficiency virus type-1 (HIV-1)-associated neurocognitive disorders (HAND; Heaton et al., 2011). HIV-1 proteins, such as the transactivator of transcription (Tat), likely contribute to synaptodendritic injury (Kruman et al., 1998; Haughey et al., 1999, 2001; Bertrand et al., 2013, 2014), as seen in Tat transgenic mice (Fitting et al., 2010, 2013), which also display neurobehavioral impairments corresponding with a HAND-associated phenotype (Carey et al., 2012; Fitting et al., 2013; Paris et al., 2014; Hahn et al, 2014).

Tat has been shown to activate glutamatergic NMDA receptors (NMDARs) through a variety of direct and indirect mechanisms (Magnuson et al., 1995; Haughey et al., 2001; Pérez et al., 2001; Li et al., 2008; Aksenov et al., 2012). Tat mediates neurotoxic glutamate release, which activates AMPA receptors (AMPARs) that can upregulate NMDA-mediated toxicity (Longordo et al., 2006), leading to dendritic structural and functional defects observed in HIV-1 infected individuals (Mattson et al., 2005). In addition to NMDAR-mediated increases in Ca^{2+} influx, NMDAR channels also rapidly influx Na^+ (Yu and Salter, 1998). In fact, Na^+ likely transits the channel more rapidly than Ca^{2+} (McBain and Mayer, 1994; Dingledine et al., 1999) and

Received Dec. 22, 2013; revised July 16, 2014; accepted Aug. 11, 2014.

Author contributions: S.F., P.E.K., and K.F.H. designed research; S.F., S.Z., and W.D.M. performed research; S.F. and W.D.M. analyzed data; S.F., M.S.B., H.I.A., and K.F.H. wrote the paper.

This work was supported by the National Institute on Drug Abuse (NIDA R01 DA018633, R01 DA033200, K02 DA027374, K99 DA033878).

The authors declare no competing financial interests.

Correspondence should be addressed to Dr Sylvia Fitting, Departments of Pharmacology and Toxicology, Virginia Commonwealth University, Richmond, VA 23298. E-mail: sfitting@vcu.edu.

DOI:10.1523/JNEUROSCI.5351-13.2014

 0270-6474/14/3412850-15$15.00/0

intracellular Na^+ ($[Na^+]_i$) can direct Ca^{2+} entry through NMDAR channels (Yu and Salter, 1998; Yu, 2006; Vander Jagt et al., 2008) by modulating NMDAR gating and expression levels (Xin et al., 2005).

Extended NMDA exposure has been shown to elevate $[Na^+]_i$ leading to ionic imbalances and ATP depletion with an accompanying loss in cellular energetics and resultant dysregulation of $[Ca^{2+}]_i$ (Vander Jagt et al., 2008). Previous studies suggest that the onset of synaptodendritic injury manifests as focal swellings or varicosities caused by excitotoxic influxes of Na^+ and/or Ca^{2+}, compensatory increases in Na^+/K^+-dependent ATPase activity, and a rapid loss in ATP mobilization (Perry et al., 2005; Greenwood and Connolly, 2007).

Clinical evidence suggests that opioid abuse can exacerbate neuro-acquired immunodeficiency syndrome (neuroAIDS; Bell et al., 1998; Nath et al., 1999; Anthony et al., 2008; Byrd et al., 2011), and experimental models support these findings by demonstrating heightened synaptodendritic degeneration with opioid and Tat coexposure (Fitting et al., 2010). The mechanisms by which opiates per se act to enhance HIV-1-induced synaptodendritic injury remain largely undefined.

The present study examined the effects of opioids on the initial events by which Tat triggers excitotoxic neuronal injury. Results indicate Tat-induced rapid Na^+ influx, $[Ca^{2+}]_i$ destabilization, and mitochondrial hyperpolarization in dendrites through excitotoxic glutamatergic mechanisms largely mediated by NMDARs. Morphine, acting via μ-opioid receptors (MORs), exacerbated this process by destabilizing mitochondrial inner membrane potential and by exacerbating $[Ca^{2+}]_i$ mobilization from internal stores through a ryanodine receptor-dependent mechanism. The results herein provide evidence that opiates exacerbate Tat-induced dendritic injury through MOR-dependent focal disruption of Ca^{2+} mobilization and mitochondrial destabilization that converge with Tat-induced excitotoxic signaling via NMDARs.

Materials and Methods

Experiments were conducted in accordance with the NIH *Guide for the Care and Use of Laboratory Animals*. All procedures were approved by the Virginia Commonwealth University Institutional Animal Care and Use Committee.

Primary neuron culture. Dissociated striatal neuronal cultures (96% neurons, 4% glia) were prepared from embryonic day 15–16 ICR (CD-1) outbred or MOR knock-out mouse embryos as previously described (Gurwell et al., 2001). The MOR knock-out mouse has been well characterized (Matthes et al., 1996; Martin et al., 2003; Chefer et al., 2009; Burbassi et al., 2010; Laurent et al., 2012). The ability of morphine to increase the neurotoxic effects of Tat are absent in striatal cells from this MOR-null strain (Zou et al., 2011). The striatum was dissected, minced, and incubated (30 min, 37°C) with trypsin (2.5 mg/ml) and DNase (0.015 mg/ml) in neurobasal medium (Invitrogen) supplemented with B27 (Invitrogen), L-glutamine (0.5 mM; Invitrogen), glutamate (25 mM; Sigma-Aldrich), and an antibiotic mixture (Invitrogen). Tissues were triturated, filtered through 70-μm-pore nylon mesh and then plated on 35 mm Petri dishes (25×10^5 neurons/dish) with 10 mm glass-bottom inserts (MatTek). The glass-bottom Petri dishes were coated with poly-L-lysine (Sigma-Aldrich) and cells were maintained in neurobasal medium supplemented with B27 (Invitrogen), 0.5 mM L-glutamine, 0.025 mM glutamate at 37°C in a humidified atmosphere containing 5% CO_2. Experiments were performed on cultures at 11–12 d *in vitro*.

Immunohistochemistry. Striatal neuron cultures were fixed in 4% paraformaldehyde for 10 min, and then permeabilized with Triton X-100 for 15 min. Mature medium spiny neurons were double- stained for GluR1 (goat, MyBioSource, aa264–277; 1:100) and GluN2B (mouse, NeuroMab, Q00960; 1:100). Primary antibodies were detected using appropriate secondary antibodies conjugated to either AlexaFluor 488 or AlexaFluor 594, respectively. Cell nuclei were visualized with Hoechst 33342. Confocal immunofluorescent images were acquired using a Zeiss LSM 700 laser scanning confocal microscope configured to an Axio Observer Z.1 microscope, and processed using Zen 2010 software (Carl Zeiss). Multiple *z*-stacks were acquired and compressed into single projected images to better show the cells in their entirety.

Assessing dendritic morphology. Striatal neuron dendritic morphology was assessed using a Zeiss Axio Observer Z.1 inverted microscope (Carl Zeiss) with an automated, computer-controlled stage encoder with environmental control (37°C, 95% humidity, 5% CO_2). For each Petri dish, six, nonoverlapping fields were randomly selected using a 63× objective. For purposes of quantification, medium spiny neurons that displayed normal morphology (Kreitzer, 2009) at the beginning of the experiment were selected from each field. Medium spiny neurons were identified in digital images of each field based on their distinctive morphology. Dendritic alterations were quantified from reconstructed confocal images that were acquired at 2 min intervals for 10 min and projected onto a single plane. Both qualitative and quantitative assessments of dendrite morphology were made. Three secondary dendrites of one neuron were randomly chosen and monitored for dendritic swelling over the 10 min assay period. Dendritic data for each neuron were averaged. Dendritic swelling was defined when the dendrite displayed aberrant features, such as beading and/or varicosity occurring along proximal and/or distal segments. An abrupt, twofold increase in the diameter of the main axis of the dendrite (typically $\geq$3 μm diameter) that did not coincide with a branch-point was used as criterion for beading or varicosity formation. Dendritic swellings were counted per 40–60 μm dendritic lengths before and every 2 min after treatment exposure on the same neuron using time-lapse imaging. Repeated-measure analyses were performed on six to eight neurons per treatment per experiment; at least three independent experiments for each treatment were conducted and presented as the mean ± SEM.

Calcium, sodium, and mitochondrial imaging. Fluorescence measurements were conducted on striatal neuron cultures using a Zeiss Axio Observer Z.1 inverted microscope (Carl Zeiss, 20× objective) with an automated, computer-controlled stage encoder with environmental control (37°C, 95% humidity, 5% CO_2). Indicators SBFI-AM (10 μM, Invitrogen) for measuring $[Na^+]_i$, rhodamine 123 (rhod123, 10 μM; Sigma-Aldrich) for measuring changes in mitochondrial inner membrane potential, and fura2-AM (2.5 μM, Invitrogen) for measuring $[Ca^{2+}]_i$, were used in Hank's balanced salt solution (HBSS; with Ca^{2+}, Invitrogen) with HEPES (10 mM, Invitrogen) and according to the manufacturer's instructions. Using Axio Vision 4.8 software, images were acquired with a MRm digital camera (Carl Zeiss) at a frame rate of 1 Hz during the first 90 s, 0.2 Hz during the next 60 s, 0.033 Hz from 2.5 min to 10 min, and 0.0166 Hz from 10 to 60 min.

For measuring $[Na^+]_i$ and $[Ca^{2+}]_i$, neurons were incubated with SBFI-AM or fura2-AM, respectively, and relative fluorescence ratio images were acquired at 340/380 nm excitation and 510 nm emission wavelengths. Conversion to $[Ca^{2+}]_i$ was calculated according to an equation described previously (Grynkiewicz et al., 1985).

For measuring changes in mitochondrial inner membrane potential, rhod123 was excited at 488 nm and the emitted fluorescence was filtered through a 515–575 nm filter. Previous studies demonstrated a Tat-induced loss in rhod123 fluorescence intensity, indicating mitochondrial hyperpolarization (Norman et al., 2007, 2008). Carbonyl cyanide 4 (trifluoromethoxy) phenylhydrazone (5 μM) was used as a positive control at the end of each experiment, which caused an expected, characteristic unquenching (depolarization of $\Delta\Psi_m$) response (data not shown; Norman et al., 2008; Perry et al., 2011). The rhod123 results are presented as mean fluorescence intensity.

The cytoplasm of neuronal perikarya was manually outlined as the region-of-interest (ROI) excluding the area over the nuclei. When imaging the dendrites, the ROI was a circle (3 μm^2) that was held to a constant size across dendrites in all experiments. The ROI for each

dendrite was selected from regions approximately one-fourth (proximal) or three-fourths (distal) along the total length of the dendrite from the soma. Data from nine dendrites from three neurons were collected in at least three experiments using neurons from separate mice. Due to the heterogeneity among neurons, the mean ± SEM values for changes in $[Na^+]_i$, $[Ca^{2+}]_i$, and rhod123 levels were computed comparing individual neurons before and at specific intervals during treatment using a repeated-measure ANOVA. Quantitative analyses of $[Na^+]_i$, $[Ca^{2+}]_i$, and rhod123 levels in neuronal perikarya or dendrites were performed on 10–20 neurons per treatment per experiment; at least three independent experiments were conducted for each treatment group.

Treatments. Treatments included HIV-1 $Tat_{1–86}$ (10–100 nM, ImmunoDiagnostics; clade B), HIV-1 $Tat_{\Delta 31–61}$ (100 nM mutant Tat), a deletion mutation lacking the excitotoxic core and basic domains (Nath et al., 1996), glutamate (5–500 μM, Tocris Bioscience), AMPA (25–100 μM, Tocris Bioscience), and morphine sulfate (500 nM, Sigma-Aldrich). Tat concentrations were chosen from the range that elicited functional deficits in glia and neurons similar to those occurring in HIV-1, and that are considered to reflect levels seen under pathological conditions (Kruman et al., 1998; Nath et al., 1999; Singh et al., 2004; El-Hage et al., 2005, 2008; Perry et al., 2010). Glutamate and AMPA concentrations were selected so that they spanned the minimal and maximal effects observed in previous studies (Marin et al., 1993; Pepponi et al., 2009; Ruiz et al., 2012) and in our preliminary experiments (data not shown). The morphine concentration used was based on our previous studies (Podhaizer et al., 2012; Suzuki et al., 2011; Zou et al., 2011) and was chosen to maximally stimulate MOR. Tat and/or drug combinations were added concurrently to the cultures, while readings were taken from the soma or dendrites for all imaging studies and from the dendrites for the morphological studies. Inhibitors/antagonists were added to the culture 30 min before, and for the duration of the experiment, except for the NMDA receptor blocker dizocilpine (MK-801, 20 μM, Tocris Bioscience) that was added right after the treatments. Pretreatment concentrations were chosen to maximally block treatments based on preliminary explorative assessments conducted before the main experiments (data not shown). Pretreatments included the: AMPA receptor antagonist CNQX (5 μM, Tocris Bioscience), opioid receptor antagonist naloxone (1.5 μM, Sigma-Aldrich), μ-opioid receptor antagonist D-Phe-Cys-Tyr-D-Trp-Arg-Thr-Pen-Thr-NH_2 (CTAP; 500 nM, Tocris Bioscience), δ-opioid receptor (DOR) antagonist naltrindole (1 μM, Tocris Bioscience), κ-opioid receptor (KOR) antagonist nor-binaltorphimine (nor-BNI; 1 μM, Tocris Bioscience), L-type calcium channel blocker nimodipine (50 μM, Tocris Bioscience), endoplasmic reticulum calcium release inhibitors dantrolene (5 μM, Tocris Bioscience) or ryanodine (1 μM, Tocris Bioscience), and pyruvate (10 mM, Sigma-Aldrich), which is rapidly metabolized to ATP (Krisher and Prather, 2012). Reagent stocks were stored at −80°C for <1 month. For the experimental manipulation of Ca^{2+}-free medium, HBSS with calcium was switched to Ca^{2+}-free HBSS medium (Invitrogen). For the experimental manipulation of low sodium in the external solution, HBSS with calcium was used but 50% of sodium bicarbonate was substituted with lithium (Li^+, Sigma-Aldrich).

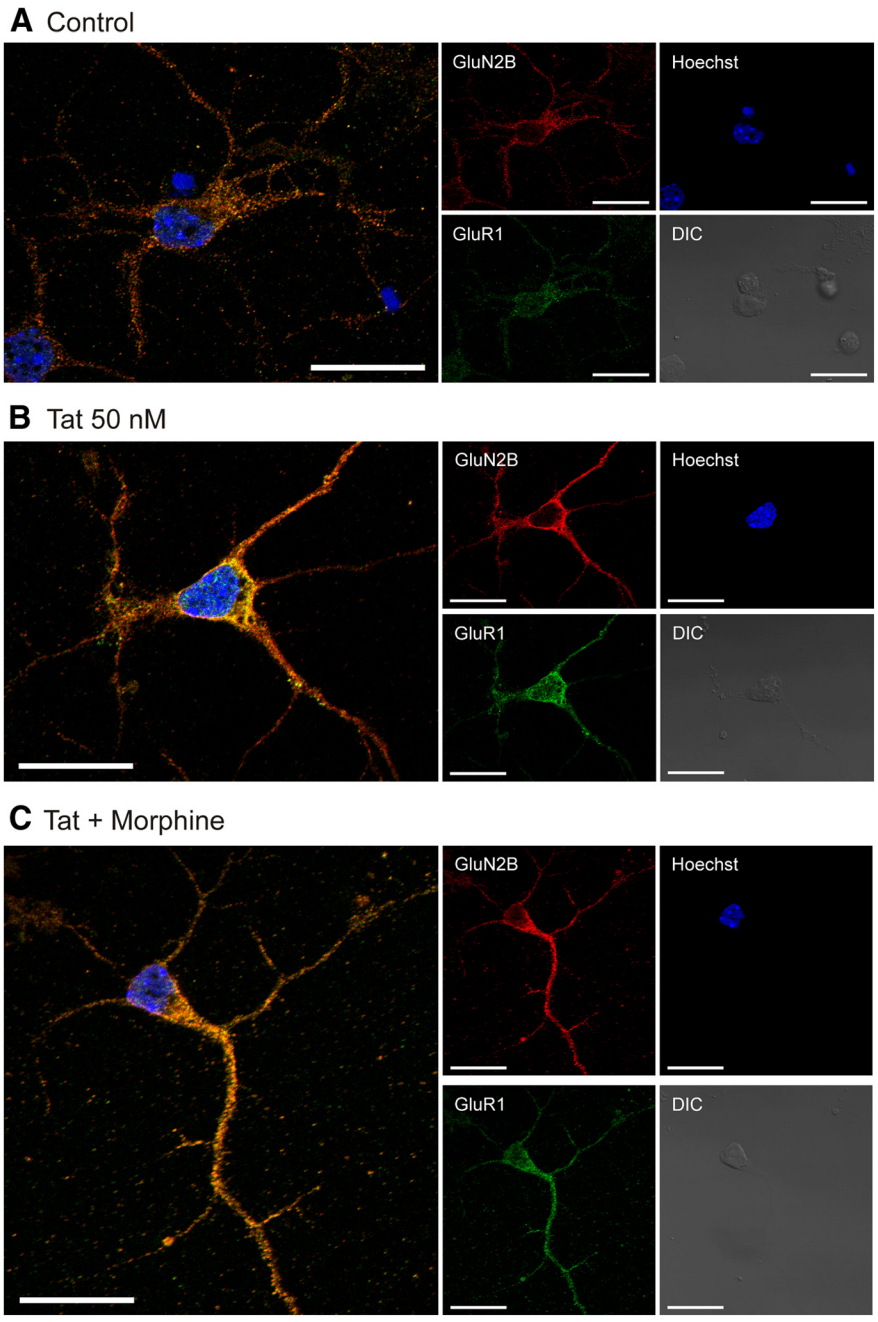

Figure 1. GluR1 (green) and GluN2B (red) receptor subunits are distributed to varying degrees throughout the cell body and dendrites of primary murine striatal medium spiny neurons. Cells were exposed to treatments for 1 h via bath application. Immunohistochemistry indicates no differences in receptor distribution for (***A***) controls, (***B***) Tat 50 nM, and (***C***) Tat (50 nM) + morphine (500 nM). Multiple *z*-stacks were projected into a single image plane to show the distribution of receptors throughout the neuron; Hoechst 33342 counterstained nuclei (blue). DIC, Differential interference contrast. Scale bars, 20 μm.

Statistical analyses. Data were analyzed using ANOVA (SYSTAT 11.0 for Windows) followed by *post hoc* tests, using Bonferroni's correction as needed. In repeated-measures ANOVAs for the within-subjects factors (i.e., comparing multiple time points), violations of compound symmetry were addressed by using the Greenhouse–Geisser degrees-of-freedom correction factor (Greenhouse and Geisser, 1959). An α level of $p < 0.05$ was considered significant for all statistical tests used. Data are expressed as the mean ± SEM from at least three independent experiments.

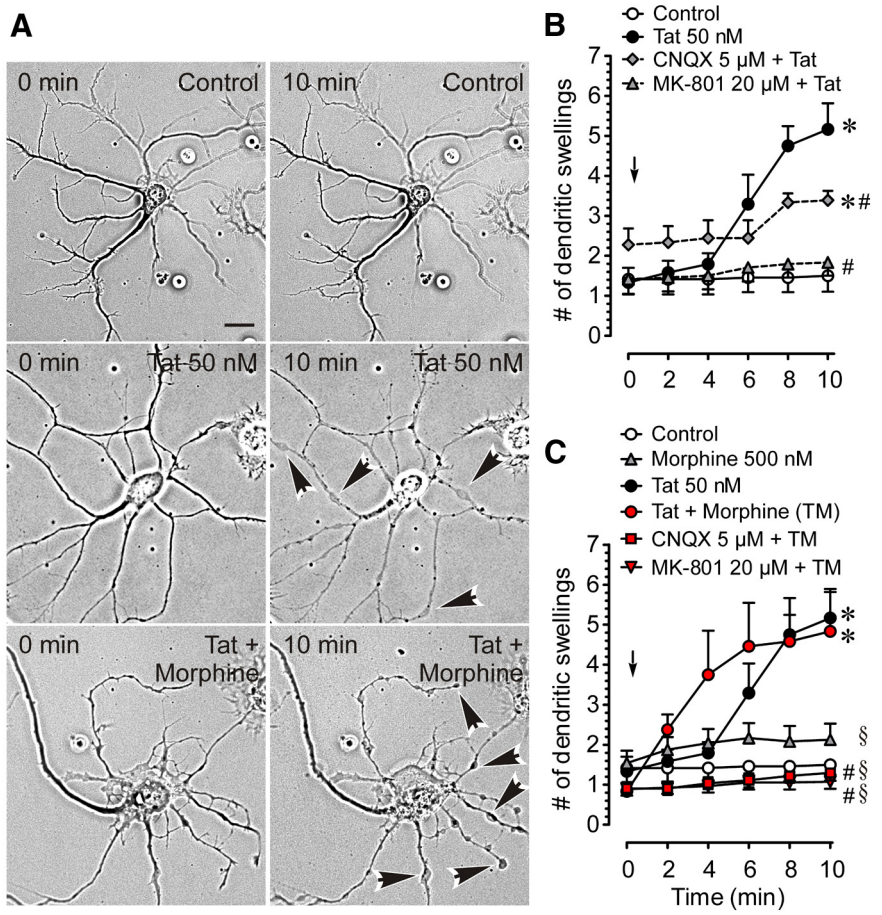

Figure 2. Time-dependent effects of Tat ± morphine on dendritic morphology in striatal medium spiny neurons. ***A***, Neurons display focal dendritic swellings/varicosities at 10 min following bath application of Tat (50 nM) ± morphine (500 nM; arrows), whereas controls show normal morphology. ***B***, ***C***, Tat significantly increases dendritic swelling after 6 min of treatment, whereas combined Tat and morphine-induced increases in dendritic swellings occur earlier at ~4 min. Tat- and combined Tat- and morphine-dependent increases in dendritic swellings were antagonized by coadministering MK-801 (20 μM) and CNQX (5 μM). Significance was assessed by ANOVA followed by Bonferroni's *post hoc* test; *$p < 0.05$ versus control, #$p < 0.05$ versus Tat 50 nM, §$p < 0.05$ versus Tat + morphine; arrows indicate the onset of Tat ± morphine treatment (3 independent experiments, 6–8 neurons per experiment). Images represent the projection of *z*-stack images acquired by microscopy at indicated times. Images are the same magnification. Scale bar, 20 μm.

Results

GluR1 and GluN2B receptor subunit localization in striatal medium spiny neurons

AMPA and NMDA receptors are ligand gated glutamatergic ion channels that mediate the majority of fast excitatory neurotransmission at CNS synapses. The AMPAR is formed of four subunits that are thought to assemble as a dimer of dimers (Tichelaar et al., 2004). The GluR1 subunit is one of the most abundant AMPAR subunits in the striatum (Stefani et al., 1998), and GluN2B has been shown to be specifically involved in NMDA-induced excitotoxicity in striatal neurons (Lui et al., 2003). Cells were stained for endogenous GluR1 (green) and GluN2B subunits (red) and counterstained with Hoechst 33342 (blue). As depicted in Figure 1, GluR1 and GluN2B are localized in the soma and dendrites. There was no significant effect on receptor distribution after 1 h Tat or combined Tat and morphine treatment. The uniform distribution of these receptors on dendrites indicates that the glutamatergic machinery necessary for a local dendritic response was present in our cultured neurons.

Tat ± morphine-induced dendritic swelling was partially prevented by MK-801 and CNQX

Excitotoxicity is characterized by dendritic changes, including swelling, and formation of dendritic varicosities. These have been previously demonstrated *in vivo* in Tat transgenic mice (Fitting et al., 2010, 2013). Morphological analyses were performed to quantify dendritic varicosity and swelling that occurred in neurons exposed to Tat and/or morphine by a 10 min bath application (Fig. 2). Tat alone significantly altered neuronal morphology starting after 6 min exposure ($p < 0.05$ vs control; Fig. 2*B*) by triggering the appearance of dendritic varicosities and swellings. Combined Tat and morphine accelerated the formation of dendritic varicosities as significance was noted after 4 min ($p < 0.05$ vs control, Fig. 2*C*). No significant alterations were noted on neurons exposed to morphine alone. Importantly, Tat- or combined Tat- and morphine-dependent increases in dendritic swellings were antagonized by MK-801 ($p < 0.05$), and partially antagonized by CNQX (Fig. 2*B*,*C*). Although the baseline for CNQX treated cells was slightly elevated, it was not significant (Fig. 2*B*); however, this was not significantly different from controls. The elevated response may become significant with more prolonged exposure. These findings suggest that Tat-induced dendritic swellings act via NMDA or AMPA receptor-related events.

Tat ± morphine-induced dendritic swellings are accompanied by losses in ion homeostasis

NMDA receptor activation has been shown to result in substantial $[Na^+]_i$ loading, and Na^+ accumulation has been suggested to be a significant contributor to neuronal injury (Rothman, 1985; Olney et al., 1986). As Tat and combined Tat and morphine treatment increased dendritic swellings, we were interested in testing if Na^+ accumulation and mitochondrial dysfunction play a role in Tat ± morphine-induced synaptodendritic injury (Fig. 3). It has been demonstrated that demands for mitochondrial ATP synthesis, which occurs due to Na^+ extrusion, is a major contributor to subsequent dysregulation of Ca^{2+} homeostasis in cultured neurons (Nicholls et al., 2007; Vander Jagt et al., 2008). Intracellular Na^+ concentrations were investigated using the ratiometric indicator SBFI-AM (Fig. 3*A*,*B*). These studies demonstrated that Tat-induced increases ($p < 0.05$ vs control) reached a peak response at ~6 min, which remained stable until the end of the 10 min period. Combined Tat and morphine treatment showed similar effects as Tat alone ($p < 0.05$ vs control). No significant alterations were noted on neurons exposed to morphine alone. Importantly, Tat- and combined Tat- and morphine-dependent increases in $[Na^+]_i$ were antagonized by MK-801 ($p < 0.05$) or

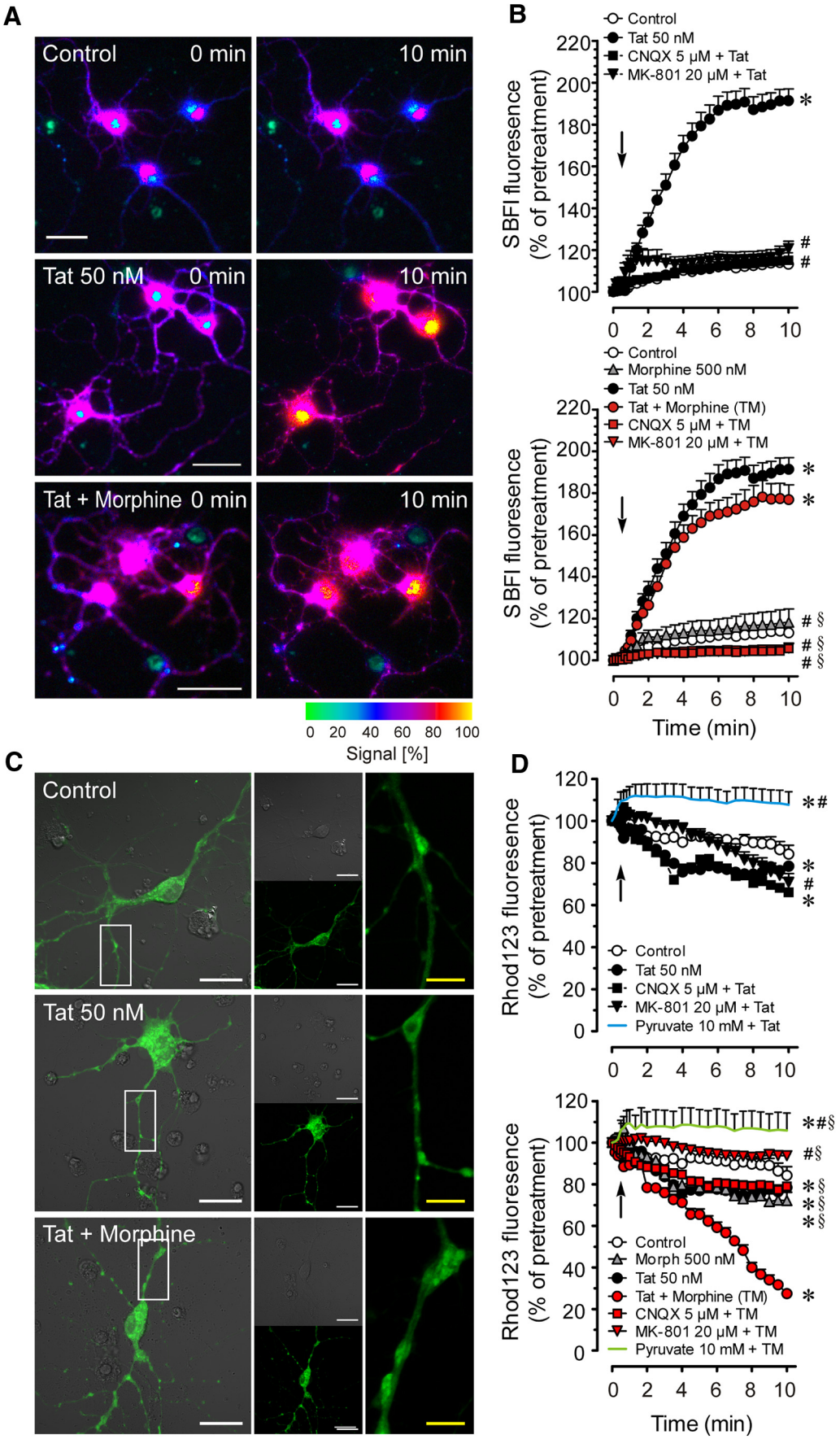

Figure 3. Tat ± morphine increases $[Na^+]_i$ and destabilizes mitochondrial inner membrane potential in striatal medium spiny neurons. ***A***, Pseudocolor images of Tat ± morphine-induced increases in $[Na^+]_i$ as assessed by ratiometric imaging of SBFI-AM. ***B***, Tat treatment alone significantly increases $[Na^+]_i$ immediately after and throughout the 10 min period (*Figure legend continues.*)

CNQX ($p < 0.05$). These data support the findings of dendritic swellings with Tat acting via AMPA and NMDA receptors.

Tat treatment alone significantly destabilized the mitochondrial inner membrane potential ($p < 0.05$ vs control), as measured by a rapid loss in rhod123 relative fluorescence (Fig. 3*C*,*D*), indicating mitochondrial hyperpolarization, and as reported previously (Norman et al., 2007, 2008). Significant synergy was seen when combined Tat and morphine treatment were compared with Tat-exposure alone ($p < 0.05$), suggesting a pronounced loss in mitochondrial inner membrane potential with coadministration of Tat and morphine. The Tat and combined Tat and morphine effects were significantly antagonized by MK-801 ($p < 0.05$) but not by CNQX (Fig. 3*D*). Pyruvate significantly reversed the effects of Tat- and combined Tat- and morphine-induced mitochondrial hyperpolarization ($p < 0.05$), indicated by an increase in rhod123 relative fluorescence (mitochondrial depolarization; Fig. 3*D*).

AMPA and NMDA receptors mediate Tat-induced increases in $[Ca^{2+}]_i$

To understand how AMPA and NMDA-related events contribute to Tat-induced dendritic swellings, the role of each receptor type in $[Ca^{2+}]_i$ changes in neurons were assessed (Fig. 4). Concentration-response curves revealed that bath exposure to Tat, AMPA, or glutamate for 10 min significantly increased $[Ca^{2+}]_i$ compared with baseline or morphine exposure ($p < 0.05$; Fig. 4*A–C*). A near exponential increase in $[Ca^{2+}]_i$ was noted immediately following Tat exposure, while a more linear increase in $[Ca^{2+}]_i$ occurred with AMPAR activation, with a more constant $[Ca^{2+}]_i$ induction across a range of glutamate concentrations. A comparison across concentrations for each treatment demonstrated significantly higher $[Ca^{2+}]_i$ following Tat treatment compared with AMPA or glutamate exposure (Fig. 4*D–F*). No difference was noted between AMPA and glutamate-induced $[Ca^{2+}]_i$ levels. In combination with morphine (500 nM), there were significant interactions depending on the particular treatment and concentration used (Fig. 4*D–F*). Interestingly, AMPA activation appears to be responsible for the initial increase in $[Ca^{2+}]_i$ (Fig. 4*E*). For example, (1) AMPA exposure rapidly triggered an initial spike in $[Ca^{2+}]_i$, and (2) the initial, but not sustained (>3 min), raise in $[Ca^{2+}]_i$ caused by Tat was significantly attenuated by CNQX coadministration ($p < 0.05$; Fig. 4*G*). Glutamate, in turn, demonstrated (1) a more sustained $[Ca^{2+}]_i$ mobilization over the 10 min time window (Fig. 4*F*), and (2) the sustained increases in $[Ca^{2+}]_i$ mediated by Tat ± morphine $[Ca^{2+}]_i$ were antagonized by MK-801 ($p < 0.05$; Fig. 4*G*,*H*), suggesting that Tat increased Ca^{2+} conductance through NMDAR channels. Partial involvement of AMPAR activation has been shown to contribute to Tat excitotoxicity downstream of NMDAR activation (Nath et al., 1996). Tat-induced neuronal excitability may be secondarily mediated by non-NMDARs, as responses mediated by NMDA receptors are rapidly desensitizing. This is in contrast to those mediated by kainate-activated non-NMDARs that are non-desensitizing (Cheng et al., 1998). Interestingly, the present study indicates that AMPA, by itself, appeared to have some effect on the initial increase in $[Ca^{2+}]_i$, whereas glutamate produced a more sustained, but more modest increases in $[Ca^{2+}]_i$ mobilization. Whether Tat-mediated AMPAR activation proceeded or initiated NMDAR activation has not been fully elucidated and requires further and more detailed studies.

Tat + morphine-induced increases in $[Ca^{2+}]_i$ are mediated via MOR

To understand the effects of combined Tat and morphine on cytosolic Ca^{2+} concentration in striatal neurons, we investigated Tat plus morphine-induced $[Ca^{2+}]_i$ responses in the presence of different opioid receptor antagonists (Fig. 5). Importantly, Tat-induced increases in $[Ca^{2+}]_i$ were significantly exacerbated for combined Tat and morphine treatment throughout an entire 30 min assessment period ($p < 0.05$; Fig. 5*A*,*B*). Naloxone was able to partially antagonize combined Tat and morphine-exacerbated responses for the first 20 min ($p < 0.05$), but failed to significantly reduce $[Ca^{2+}]_i$ for the last 10 min during assessment (Fig. 5*D*). As naloxone has high affinity for MOR, but also some affinity for DOR and KOR, we were interested in determining whether a non-MOR might contribute to the combined effects of morphine and Tat-induced exacerbation of $[Ca^{2+}]_i$. Accordingly, pharmacological strategies were used to manipulate opioid receptor-mediated pathways. Interestingly, neither nor-BNI, a KOR antagonist, nor naltrindole, a DOR antagonist affected the combined Tat and morphine-induced increases in $[Ca^{2+}]_i$ (Fig. 5*B*,*D*). In contrast, the specific MOR antagonist CTAP significantly decreased combined Tat and morphine-induced $[Ca^{2+}]_i$ ($p < 0.05$; Fig. 5*B*). Further, striatal neuron cultures from MOR knock-out mice failed to show interactive increases in $[Ca^{2+}]_i$ following combined Tat and morphine treatment compared with Tat-exposure alone (Fig. 5*C*,*D*).

Tat + morphine-induced increases in $[Ca^{2+}]_i$ were blocked by ryanodine and pyruvate, whereas increases in $[Na^+]_i$ were attenuated by pyruvate only

We used pharmacological strategies to determine the sources of combined Tat and morphine-driven increases in $[Ca^{2+}]_i$ and $[Na^+]_i$ (Fig. 6). L-type calcium channels were blocked with nimodipine to test whether the increase of $[Ca^{2+}]_i$ resulted from increased L-type voltage-gated Ca^{2+} channel activation. The ryanodine receptor (RyR) antagonists, dantrolene, and ryanodine, were individually used to test for the involvement of intracellular calcium stores. Pyruvate was used to assess the involvement of ATP depletion due to increases in Na^+/K^+-dependent ATPase activity. Importantly, Tat- and morphine-induced increases in $[Ca^{2+}]_i$ transients were attenuated by blockade of RyR ($p < 0.05$), and partially blocked by pyruvate, indicating the importance of intracellular calcium stores and ATP levels (Fig. 6*A*,*B*). Even though nimodipine did not significantly attenuate increased $[Ca^{2+}]_i$ mobilization (Fig. 6*A*,*B*), Ca^{2+}-free medium or low $[Na^+]_o$ significantly decreased $[Ca^{2+}]_i$ despite combined

←

(*Figure legend continued.*) following exposure. Tat- and combined Tat and morphine-induced $[Na^+]_i$ increases were markedly reduced by coadministering MK-801 and CNQX. $[Na^+]_i$ was unaffected by exposure to morphine, whereas combined Tat and morphine treatment did not differ from Tat alone. ***C***, Confocal images of rhod123 fluorescence (an index of inner mitochondrial membrane potential) were taken for control, Tat 50 nM, and Tat + morphine treated cells (10 min treatment exposure). ***D***, Tat and combined Tat- and morphine-induced decreases in rhod123 fluorescence intensity were markedly attenuated by MK-801, but not CNQX. Rhod123 fluorescence intensity was unaffected by morphine, whereas a synergistic decline in fluorescence was seen with combined Tat and morphine treatment, indicating mitochondrial hyperpolarization. Incubation with pyruvate for 30 min before Tat, and combined Tat and morphine treatments resulted in the inhibition of rhod123 signal with mitochondrial depolarization. Significance was assessed by ANOVA followed by Bonferroni's *post hoc* test; *$p < 0.05$ versus control, #$p < 0.05$ versus Tat 50 nM, §$p < 0.05$ versus Tat + morphine; arrows indicate the onset of Tat ± morphine treatment (3 independent experiments, 10–20 neurons per experiment). Images are the same magnification. Scale bars: white, 20 μm; yellow, 5 μm. Morph, Morphine.

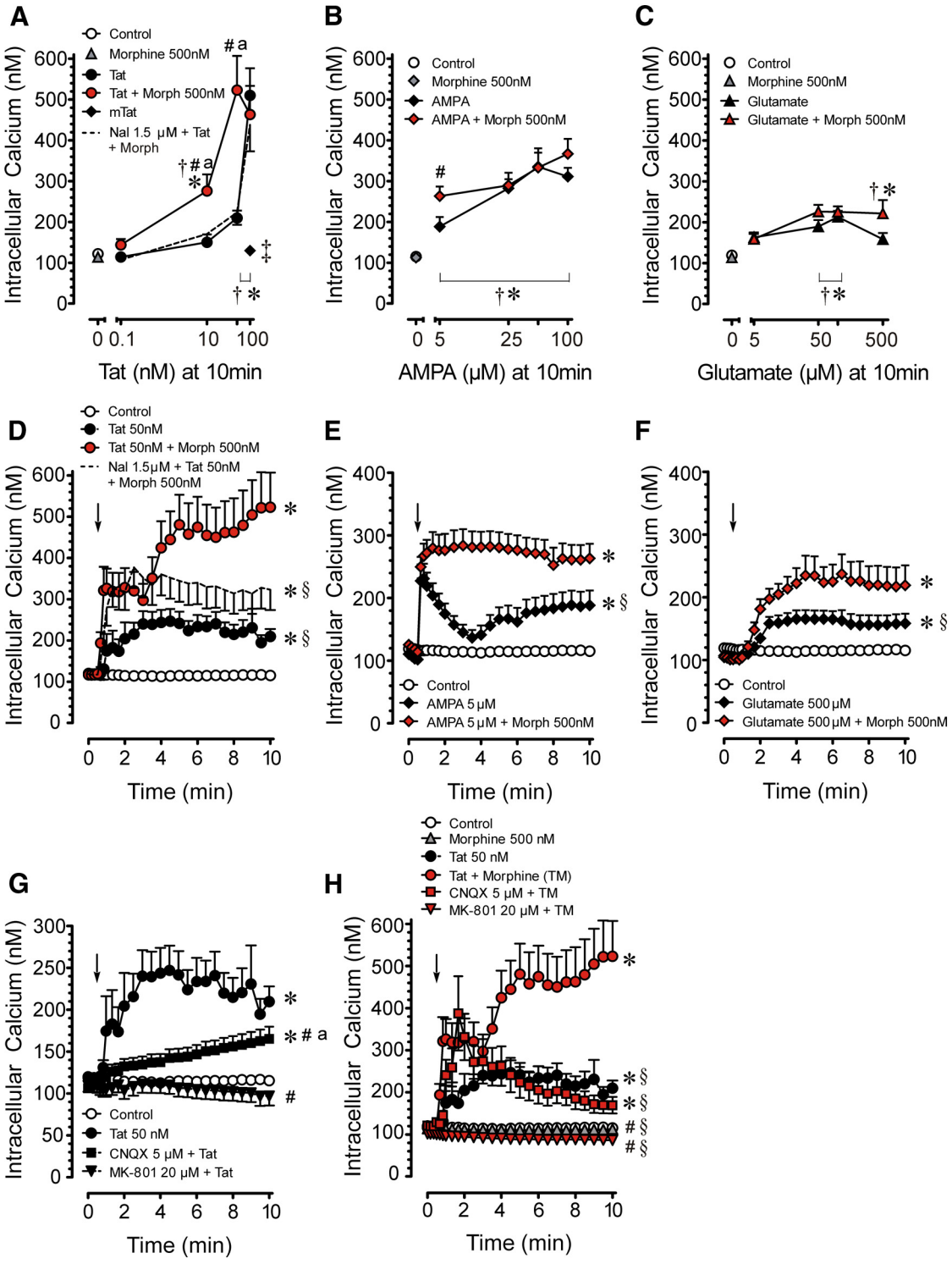

Figure 4. AMPA and NMDA receptors are involved in Tat-induced increases in $[Ca^{2+}]_i$. ***A–C***, Concentration-dependent effects of bath applied Tat, AMPA, or glutamate on $[Ca^{2+}]_i$. ***A***, Tat concentrations >50 nM increase $[Ca^{2+}]_i$, whereas the inactive, $Tat_{\Delta 31-61}$ mutant Tat (mTat; 100 nM) and morphine had no effect. Combined Tat (10 or 50 nM) and morphine (500 nM) exacerbate increases in $[Ca^{2+}]_i$ compared with equimolar concentrations of Tat alone, which is markedly reduced by coadministering naloxone, indicating the response is mediated by opioid receptors. ***B***, AMPA significantly increases $[Ca^{2+}]_i$ in a concentration-dependent manner; concurrent morphine administration selectively significantly enhanced increases in $[Ca^{2+}]_i$ at 5 μM concentrations of AMPA. ***C***, Glutamate significantly increases $[Ca^{2+}]_i$ at intermediate concentrations, but the $[Ca^{2+}]_i$ increases are unaffected by concurrent morphine exposure. ***D–F***, Tat, AMPA, and glutamate each interact uniquely with morphine. ***D***, Tat increases $[Ca^{2+}]_i$. Tat-induced $[Ca^{2+}]_i$ increases are exacerbated by morphine and the response is sustained throughout the 10 min period following exposure. ***E***, AMPA increases $[Ca^{2+}]_i$ only initially, whereas combined AMPA and morphine administration displays prolonged increases in $[Ca^{2+}]_i$. ***F***, Glutamate alone sustains $[Ca^{2+}]_i$, which is partially exacerbated in combination with morphine. ***G***, ***H***, Importantly, Tat and combined Tat- and morphine-induced $[Ca^{2+}]_i$ increases were partially or completely antagonized by CNQX or MK-801, respectively. Statistical significance was assessed by ANOVA followed by Bonferroni's *post hoc* test; $*p < 0.05$ versus control, $\#p < 0.05$ versus Tat, $\S p < 0.05$ versus Tat + morphine; $^a p <$ 0.05 versus naloxone + Tat + morphine, $\dagger p < 0.05$ versus morphine, $\ddagger p < 0.05$ mTat versus Tat, Tat + morphine, and naloxone + Tat + morphine. The brackets indicate data with overlapping significance; arrows indicate the onset of treatment (3 independent experiments, 10–20 neurons per experiment). Nal, Naloxone; morph, morphine.

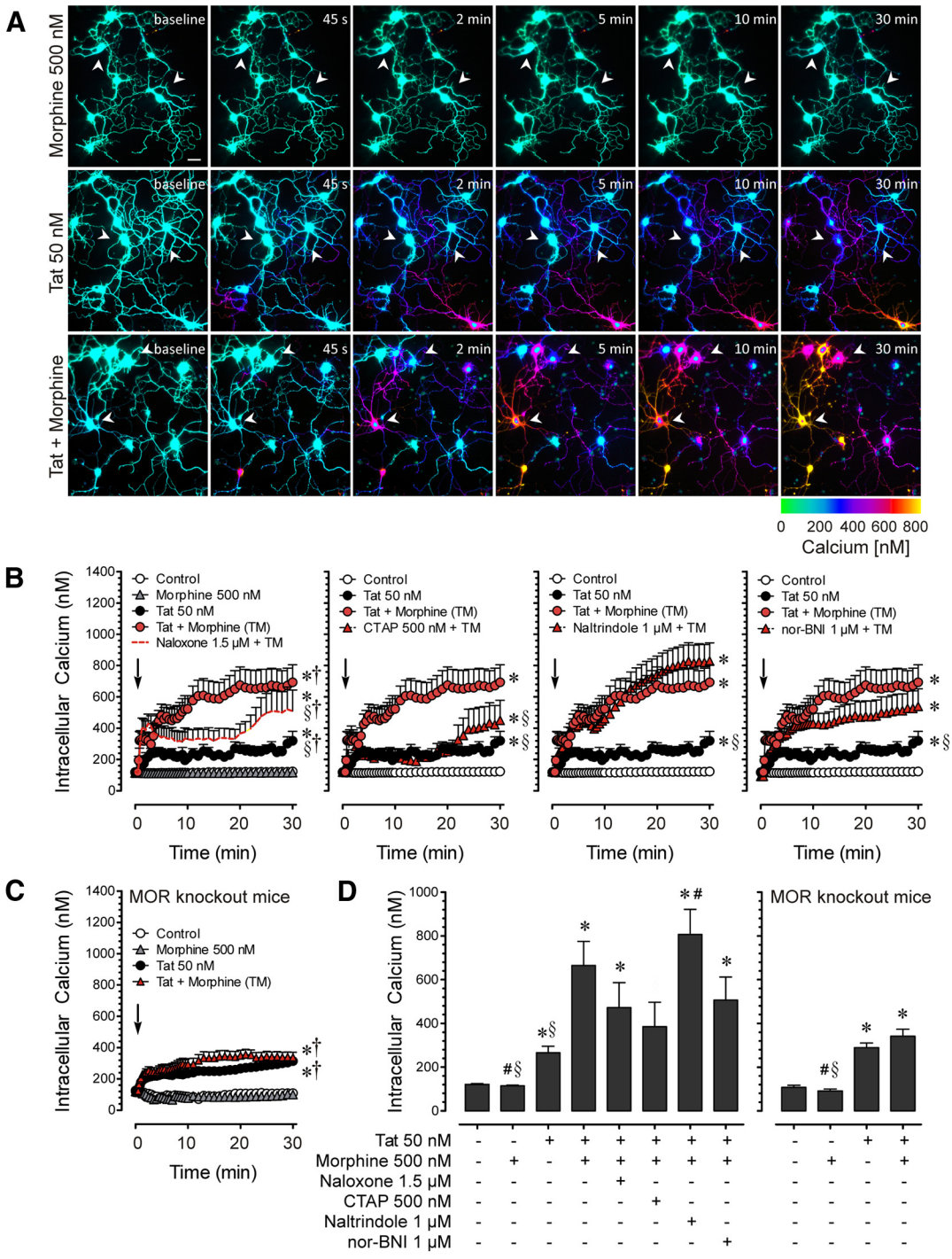

Figure 5. Morphine-dependent increases in $[Ca^{2+}]_i$ (alone or in combination with Tat) are mediated by MOR as shown with pharmacological (CTAP) and genetic (MOR knock-out mice) strategies. ***A***, Pseudocolor images of Tat- and/or morphine-induced increases in $[Ca^{2+}]_i$ as assessed by ratiometric imaging of fura 2. ***A***, ***B***, Minimal changes in $[Ca^{2+}]_i$ were seen with morphine alone (white arrowheads, top row). Alternatively, Tat by itself significantly increased $[Ca^{2+}]_i$ and morphine exacerbated the effects of Tat (white arrowheads, middle and bottom rows). In the presence of morphine, Tat-induced $[Ca^{2+}]_i$ increases were markedly reduced by coadministering naloxone or CTAP. Naltrindole or nor-BNI did not attenuate the effects of Tat and morphine coexposure, suggesting that DOR and KOR, respectively, are not involved. ***C***, Likewise, despite significant increases in $[Ca^{2+}]_i$ with Tat alone, combined Tat and morphine treatment does not further increase $[Ca^{2+}]_i$ in striatal neurons from MOR-null mice. ***D***, Average $[Ca^{2+}]_i$ during the final 10 min (from 20 to 30 min) indicate significant increases in $[Ca^{2+}]_i$ by Tat alone compared with controls, with an exacerbated response for combined Tat and morphine treatment, which is antagonized by CTAP and not seen in neurons of MOR knock-out mice. Statistical significance was assessed by ANOVA followed by Bonferroni's *post hoc* test; $*p < 0.05$ versus control, $\#p < 0.05$ versus Tat, $\S p < 0.05$ versus Tat + morphine, $\dagger p < 0.05$ versus morphine; arrows indicate the onset of treatment (3 independent experiments, 10–20 neurons per experiment). TM, Tat 50 nM + morphine 500 nM. Images are the same magnification. Scale bar, 20 μm.

Tat and morphine treatment ($p < 0.05$), but not for Tat treatment alone (Fig. 6*C*,*D*). Ca^{2+} influx was mostly, but not completely, blocked with Ca^{2+}-free medium ($[Ca^{2+}]_o$) for several likely reasons. Despite the use of Ca^{2+}-free medium, in the absence of chelators (e.g., EGTA, EDTA), there is always some Ca^{2+} present. The reason for this is that small amounts of Ca^{2+} ions are released extracellularly via (1) transporter efflux (e.g., plasma membrane Ca^{2+}-ATPase) from normal cells, (2) injured/dying

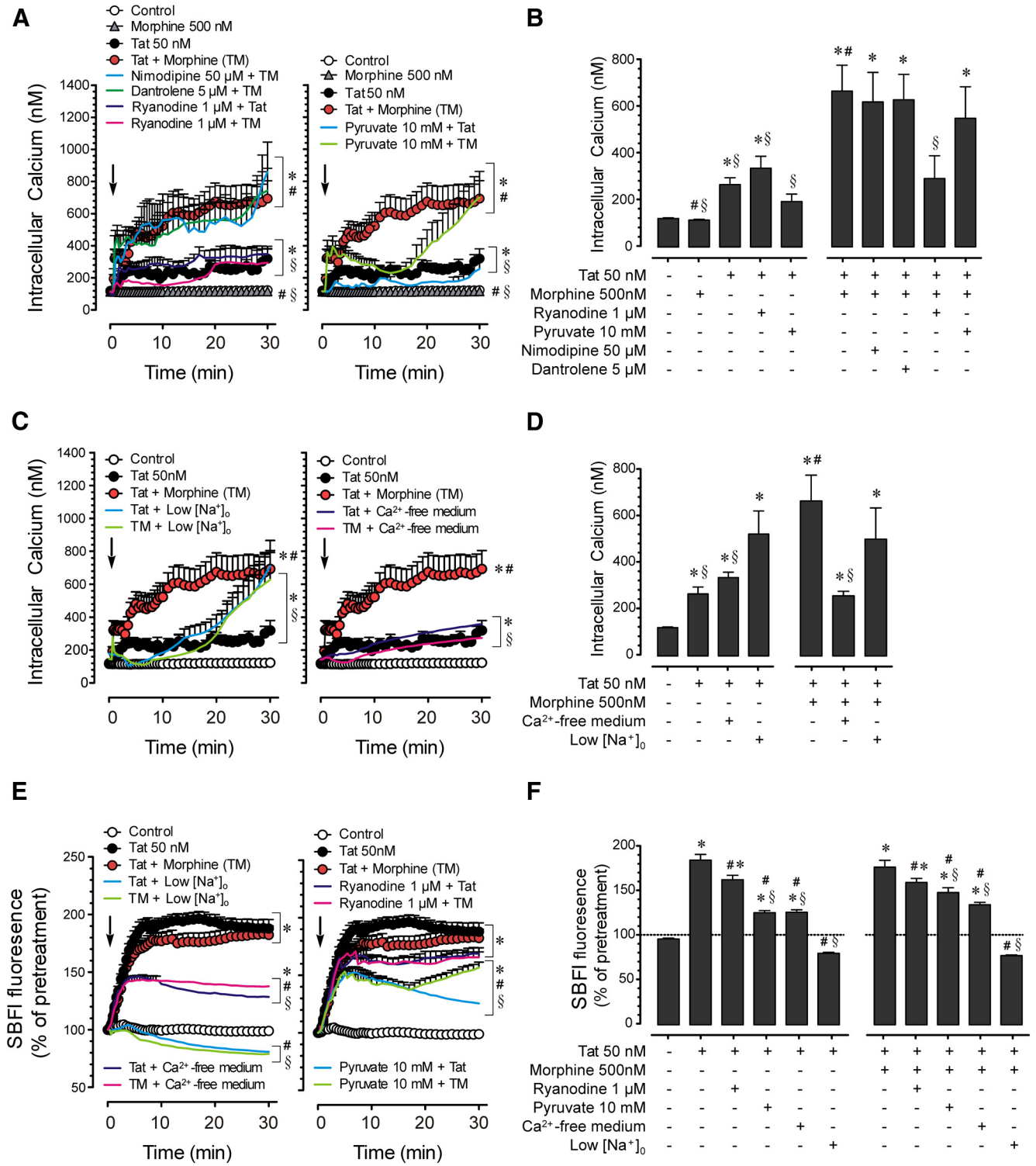

Figure 6. Effects of morphine and/or Tat on $[Ca^{2+}]_i$ and $[Na^+]_i$ in neuronal dendrites following 0–30 min exposure. ***A***, Acute Tat + morphine-induced increases in $[Ca^{2+}]_i$ are attenuated by ryanodine or pyruvate, while nimodipine (L-type Ca^{2+} channel blocker) and dantrolene do not show any effects on Tat ± morphine-induced changes in $[Ca^{2+}]_i$. ***B***, Average $[Ca^{2+}]_i$ during the final 10 min (from 20 to 30 min) indicate ryanodine significantly blocks combined Tat and morphine-induced increases in $[Ca^{2+}]_i$, whereas no effects are noted for nimodipine, dantrolene, or pyruvate. ***C***, Ca^{2+}-free medium or low $[Na^+]_o$ significantly decreases Tat plus morphine increases in $[Ca^{2+}]_i$. However, Ca^{2+}-free or low Na^+ medium significantly decreases $[Ca^{2+}]_i$ following Tat treatment alone, but Tat increases are exacerbated after 20 min. ***D***, Tat + morphine-induced increases in $[Ca^{2+}]_i$ during the interval from 20 to 30 min are significantly reduced by Ca^{2+}-free medium. ***E***, Tat ± morphine similarly increases $[Na^+]_i$, which is completely blocked by low $[Na^+]_o$. Although Ca^{2+}-free medium attenuates the Tat ± morphine-associated elevations in $[Na^+]_i$, $[Na^+]_i$ levels remained markedly above baseline levels perhaps suggesting some Ca^{2+} efflux from internal stores. Exogenous pyruvate also significantly attenuate Tat ± morphine-induced increases in $[Na^+]_i$, whereas ryanodine has no effect. ***F***, Average $[Na^+]_i$ during the final 10 min indicate a significant blockage of Tat ± morphine increases in $[Na^+]_i$ by low $[Na^+]_o$, with partial reductions in $[Na^+]_i$ following exposure to Ca^{2+}-free medium or exogenous pyruvate, but not ryanodine. Statistical significance was assessed by ANOVA followed by Bonferroni's *post hoc* test; $^*p < 0.05$ versus control, $\#p < 0.05$ versus Tat, $\S p < 0.05$ versus Tat + morphine; arrows indicate the onset of treatment (3 independent experiments, 10–20 neurons per experiment). TM, Tat 50 nM + morphine 500 nM; low $[Na^+]_o$: 50% of the extracellular Na^+ was substituted with Li^+.

cells (e.g., from mitochondria), or (3) binding sites within the extracellular matrix. Although the use of chelators would further limit Ca^{2+} entry, chelators are incompatible with the current assay because they can promote cellular detachment from the culture dish. Thus, in the present studies, it is likely that despite the use of Ca^{2+}-free medium some Ca^{2+} was still able to enter from the extracellular space, albeit at greatly reduced levels. For Tat ± morphine-induced increases in $[Na^+]_i$, pyruvate or Ca^{2+}-free medium significantly attenuated the increases in $[Na^+]_i$ ($p < 0.05$), whereas $[Na^+]_i$ increases were unaffected by ryanodine. There was a complete blockade of $[Na^+]_i$ with low $[Na^+]_o$ ($p < 0.05$), suggesting that Na^+ transients were due to an influx of extracellular sodium (Fig. 6*E*,*F*).

Tat ± morphine-induced increases in $[Ca^{2+}]_i$ in dendrites and soma

To investigate the distribution of increases in cytosolic Ca^{2+} concentration in striatal neurons, we investigated the $[Ca^{2+}]_i$ response in the soma, as well as the dendrites following different treatments (Fig. 7). Although control and morphine treatments did not significantly elevate $[Ca^{2+}]_i$ in the soma or dendrites, exposure to Tat ± morphine increased $[Ca^{2+}]_i$ ($p < 0.05$ vs corresponding control; Fig. 7*A*–*C*). For both treatments, elevated $[Ca^{2+}]_i$ in the distal and proximal dendrites preceded and was more exaggerated than increases in the soma, and was sustained throughout the 30 min assessment period (Fig. 7*B*). Ca^{2+} overload consistently originated in the distal dendrites and propagated toward the soma, ultimately involving the entire neuron.

Discussion

The rapid and highly localized response to Tat ± morphine suggests that both interact directly with neurons. Tat can interact directly with GluN1 receptors (Cheng et al., 1998; Li et al., 2008), nonselective cation channels (Magnuson et al., 1995; Nath et al., 1996; Menegon et al., 1997; Cheng et al., 1998), and the dopamine transporter (Zhu et al., 2009; Midde et al., 2013), whereas morphine can interact directly with the dendritic spines of MOR-expressing cerebral cortical and hippocampal neurons (Liao et al., 2005, 2007). Many of these molecular targets (especially NMDARs) alter membrane properties and can rapidly depolarize neurons. Tat can act via non-NMDARs (Haughey et al., 1999, 2001). However, the nature of the non-NMDAR molecular target(s), and whether the enhanced neuronal excitability is secondary to a glial response, remains to be established. Further, it has been reported that when Tat was pressure-applied to neurons, the time to maximal $[Ca^{2+}]_i$ production in some neurons was 2–3 s, which resulted from Tat-induced Ca^{2+} mobilization from inositol 1,4,5-trisphosphate (IP_3)-regulated stores (Haughey et al., 1999). How morphine interacts with Tat to increase neuronal excitability is less certain. Morphine-dependent exacerbation of Tat neurotoxicity has been attributed to direct actions on glia (Zou et al., 2011). Although morphine typically acts in an inhibitory manner, an excitatory MOR-1K splice variant (Gris et al., 2010) has been described in human astroglia (Dever et al., 2014). In that study, MOR-1K was not found to be expressed by neurons, although the human neurons sampled were from undefined brain regions and did not appear to include striatal neurons.

In the present study, GluR1 and GluN2B antigenicity was localized to the dendrites of striatal neurons, indicating that a focal dendritic response to Tat was possible. As treatments were bath applied, we were unable to isolate dendritic or somal responses. Nevertheless, because dendritic increases in $[Ca^{2+}]_i$ were more dramatic and typically preceded changes in the soma, it infers a greater susceptibility of the dendrites to Tat ± morphine excitotoxicity. The positive trophic effects of glutamatergic receptor activation (Liu et al., 2007; Hardingham, 2009) may be overshadowed by GluN2B mediated excitotoxicity (Li et al., 2008; Eugenin et al., 2011). Tat or combined Tat and morphine exposure did not appear to redistribute glutamatergic receptors along dendrites, suggesting the focal vulnerability is not caused by local differences in NMDAR/AMPAR density.

Ca^{2+} and Na^+ influx was blocked by MK-801, a NMDAR open-channel blocker. The reason that glutamate was less potent than Tat is uncertain, but likely has to do with their distinct pharmacological and biochemical properties. Although Tat and glutamate both activate NMDARs, Tat does not appear to act at the glutamate binding site, but instead acts allosterically and seemingly noncompetitively at a site unrelated to glutamate binding (Li et al., 2008). If Tat-induced Na^+ entry is sufficiently great, Na^+ may reverse the Na^+/Ca^{2+} exchanger (NCX) promoting excitotoxic Ca^{2+} to reenter the cell (Bindokas and Miller, 1995; Yu and Choi, 1997; Wolf et al., 2001). Increased $[Na^+]_i$ can mediate the release of Ca^{2+} from mitochondria (Al-Shaikhaly et al., 1979). The effect of Tat on $[Na^+]_i$ is a relatively novel proposition. Na^+ influx has been reported to provide essential positive feedback to overcome Ca^{2+}-induced inhibition of NMDA channel gating and to exacerbate Ca^{2+} influx, potentiating Ca^{2+} conductance through NMDA channels (Xin et al., 2005; Yu, 2006). $[Na^+]_i$ can act as a signaling factor common to processes that upregulate NMDARs by non-NMDA glutamate channels, voltage-gated Na^+ channels, and remote NMDARs (Yu and Salter, 1998; Yu, 2006). The effects of Tat ± morphine appeared to be biphasic (Fig. 6*C*,*D*). During the first phase, Tat-induced increases in $[Ca^{2+}]_i$ appeared to be dependent on $[Na^+]_o$. This suggests that Na^+ influx, mediated by Tat, results in Ca^{2+} influx. The resultant Ca^{2+} influx may stimulate phospholipase C (PLC). PLC generates IP_3 and activates the protein kinase C activator diacylglycerol (Berridge, 1987; Nishizuka, 1988), which can result in an IP_3-mediated Ca^{2+} release from internal stores. In Ca^{2+}-free medium, $[Ca^{2+}]_i$ levels were unaltered, suggesting that most $[Ca^{2+}]_i$ originates from internal sources. Regarding $[Na^+]_i$, Na^+ influx occurred with Ca^{2+}-free medium, although $[Na^+]_i$ was significantly reduced, which may arise from reduced efficiency of the NCX. Moreover, when extracellular Na^+ ($[Na^+]_o$) was decreased (by substituting 50% Li^+), the initial phase of the $[Ca^{2+}]_i$ increase was reduced, suggesting that low $[Na^+]_o$ affects $[Ca^{2+}]_i$ levels. This may result from decreased Na^+-dependent Ca^{2+} release. Additionally, in the presence of Li^+, $[Ca^{2+}]_i$ is reduced and mitochondrial Ca^{2+} overload does not occur (Kiedrowski, 1999). Further, Li^+ is a noncompetitive inhibitor of inositol monophosphatase that can inactivate PLC. As expected, Na^+ influx was blocked by low $[Na^+]_o$. During the second phase, Tat mediated a sustained increase in $[Ca^{2+}]_i$ and $[Na^+]_i$ levels. When $[Ca^{2+}]_o$ was significantly reduced via Ca^{2+}-free medium, $[Ca^{2+}]_i$ was unaffected, although $[Na^+]_i$ was reduced similar to the initial phase, which likely reflected reduced efficiency of the NCX. In turn with low $[Na^+]_o$, the NCX is likely to be undergoing a reversal since $[Ca^{2+}]_i$ was enhanced during the second phase. The ability of low $[Na^+]_o$ to affect the reversal of the NCX is well recognized (Yu and Choi, 1997). Low $[Na^+]_o$ resulted in the absence of $[Na^+]_i$ increases.

With combined Tat and morphine, the events of the first phase were significantly enhanced. Moreover, the effects of combined Tat and morphine, but not Tat alone, appeared to be ryanodine-sensitive suggesting that Tat likely stimulated an IP_3-dependent pathway, as shown previously (Haughey et al., 1999).

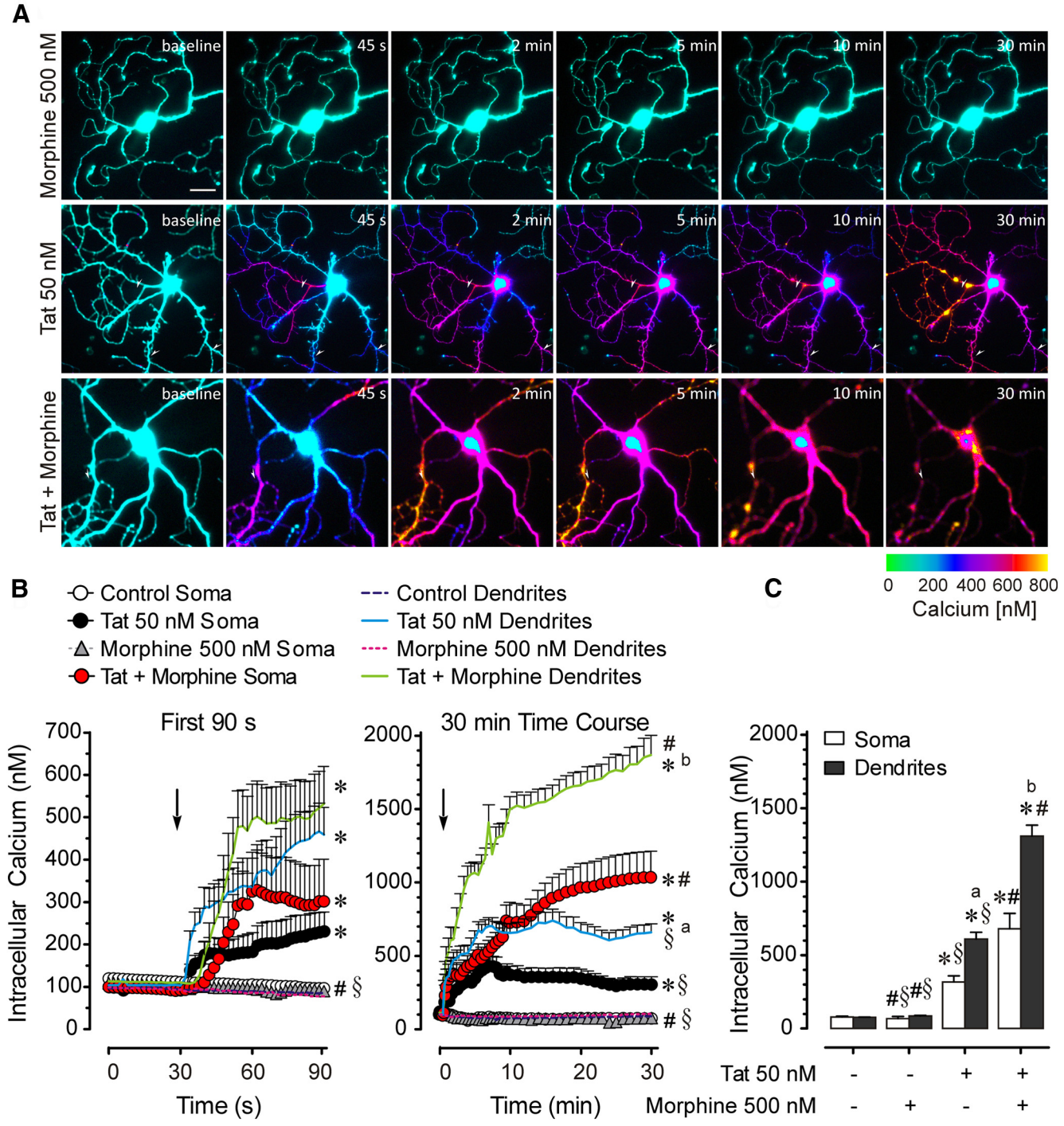

Figure 7. Tat ± morphine-induced increases in $[Ca^{2+}]_i$ are higher in dendrites compared with the soma in the same neurons. ***A***, Pseudocolor images of Tat ± morphine-induced increases in $[Ca^{2+}]_i$ show rapid elevations in $[Ca^{2+}]_i$ in the dendrites compared with soma in response to Tat ± morphine (white arrowheads). ***B***, Exposure to medium alone (control) or morphine did not affect $[Ca^{2+}]_i$ levels in the soma or dendrites. Tat ± morphine significantly increases $[Ca^{2+}]_i$, with an initial increase in $[Ca^{2+}]_i$ in the soma and dendrites that is followed by a significant elevated $[Ca^{2+}]_i$ response in dendrites (distal and proximal dendrites) compared with the soma. ***C***, Average $[Ca^{2+}]_i$ during the final 10 min indicate overall significant differences between the different treatments. Statistical significance was assessed by ANOVA followed by Bonferroni's *post hoc* test; $^*p < 0.05$ versus corresponding control, $^\#p < 0.05$ versus corresponding Tat, $^\S p < 0.05$ versus corresponding Tat + morphine, $^a p < 0.05$ versus Tat soma, $^b p < 0.05$ versus Tat + morphine soma; arrows indicate onset of treatment (3 independent experiments, 3 neurons per experiment, 9 dendrites per experiment). Images are the same magnification. Scale bar, 20 μm.

Morphine coexposure accelerated the formation of Tat-induced focal dendritic varicosities, which were accompanied by enhanced localized increases in $[Ca^{2+}]_i$ and alterations in mitochondrial inner membrane potential. $[Na^+]_i$ increases cannot be attributed to these effects since no differences were seen with Tat versus combined Tat and morphine treatment. Because NMDAR activation allows Na^+ and Ca^{2+} to enter the cell (Yu and Salter, 1998; Yu, 2006; Vander Jagt et al., 2008), our findings indicate that morphine is converging downstream of NMDARs, as combined Tat and morphine showed significantly higher $[Ca^{2+}]_i$, mobilization, whereas $[Na^+]_i$ did not increase when compared with Tat alone. This hypothesis is supported by the finding that

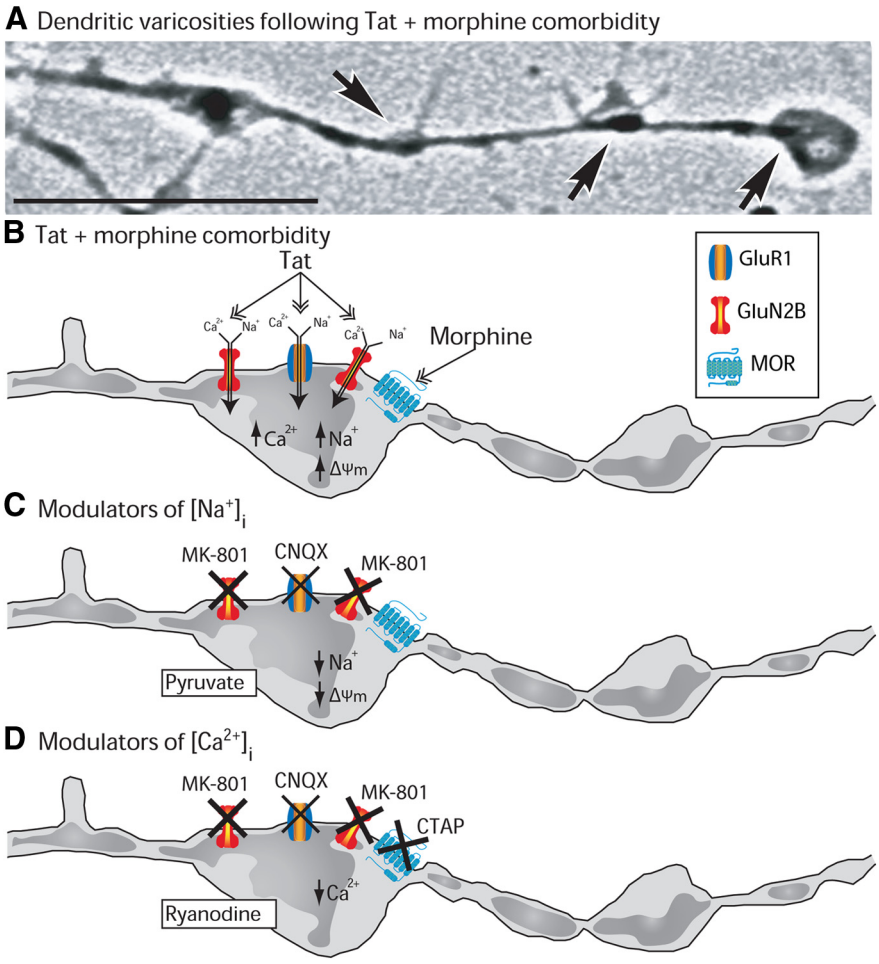

Figure 8. Theoretical model of combined Tat- and morphine-induced synaptodendritic injury. ***A***, Micrograph of a dendrite of a striatal medium spiny neuron with formation of neuronal dendritic swellings after 10 min exposure to Tat (50 nM) and morphine (500 nM; arrows). Scale bar, 20 μm. ***B***, Combined Tat and morphine promotes structural and functional defects in dendrites via AMPAR, NMDAR, and MOR, causing influxes of Na^+ and/or Ca^{2+}, compensatory increases in Na^+/K^+-dependent ATPase activity, and a rapid loss in ATP mobilization with an inability to extrude excess Na^+ via Na^+/K^+-ATPase caused by mitochondrial hyperpolarization. ***C***, Excessive $[Na^+]_i$ can be antagonized by NMDA and partially by AMPA receptor antagonists MK-801 and CNQX, respectively. Pyruvate attenuated Tat + morphine-induced increases in $[Na^+]_i$ transients, suggesting the involvement of ATP depletion due to increases in Na^+/K^+-dependent ATPase activity. ***D***, Dysregulation of $[Ca^{2+}]_i$ homeostasis by Tat + morphine appears to be mediated downstream of $[Na^+]_i$ at the level of Ca^{2+} mobilization, which in turn is likely regulated via RyR and/or IP_3, and enhanced by morphine exposure via MOR. $\Delta_{\Psi m}\downarrow$, Mitochondrial depolarization.

combined Tat and morphine-induced initial losses in ion homeostasis and increases in $[Ca^{2+}]_i$ mobilization were attenuated by the RyR inhibitor ryanodine, indicating the importance of $[Ca^{2+}]_i$ mobilization in Tat and morphine-induced synaptodendritic instability. Tat and opiates can evoke Ca^{2+} influx through NMDAR or L-type Ca^{2+} channels and can increase Ca^{2+} mobilization from IP_3-dependent stores via Ca^{2+}-induced Ca^{2+} release through RyR (Hauser et al., 1996; Kruman et al., 1998; Haughey et al., 1999; El-Hage et al., 2005, 2008). Morphine likely exacerbates the effects of Tat through excessive $[Ca^{2+}]_i$ influx and by depleting $[Ca^{2+}]_i$ from RyR-sensitive sites. Normally, there is a critical period of excitotoxic vulnerability (Mattson et al., 2008; Vander Jagt et al., 2008). If the flooding of $[Ca^{2+}]_i$ from NMDAR- and RyR-dependent sites coincides, this would exaggerate the loss in Ca^{2+} homeostasis and exacerbate neuronal injury; suggesting a mechanism by which morphine converges with Tat to further disrupt Ca^{2+} homeostasis. The particular RyR2 isoform might be important, as Tat plus morphine-induced $[Ca^{2+}]_i$ mobilization was not inhibited by dantrolene. Dantrolene inhibits Ca^{2+} release through RyR channels by specifically targeting the RyR1 and RyR3, but not the RyR2, isoform (Zhao et al., 2001). Ryanodine is highly selective for all RyR isoforms with limited effects on IP_3-mediated Ca^{2+} signaling (MacMillan et al., 2005).

The additive effects of morphine plus Tat were prevented by a MOR antagonist and were absent in MOR knock-out medium spiny neurons, suggesting the selective involvement of MORs. Moreover, neither the DOR nor the KOR antagonists prevented the neurotoxic effects of morphine, which further supports the notion that MORs primarily mediate the interactive neuropathogenesis of Tat and morphine. Last, the absence of interactive morphine toxicity in neurons from MOR-null mice suggests that opiate-dependent activation of Toll-like receptor 4 is not operative, which differs from another study (Wang et al., 2012).

The importance of MOR-AMPAR/NMDAR spatiotemporal relationships in opiate drug-HIV-1 Tat interactive neuropathogenesis has wide support from other model systems. Morphine acting via MOR converges with glutamatergic signals from AMPARs to cause dynamin-dependent MOR internalization, which triggers spine reductions (Liao et al., 2007). MOR clusters colocalize with synaptophysin and NMDARs (73 ± 8%) in hippocampal neurons in culture (Liao et al., 2007). The frequent overlap of MOR in glutamatergic synapses suggests that opioids might modulate the morphology and/or function of these synapses (Liao et al., 2005). MOR immunoreactivity is associated with approximately one-third of striatal medium spiny neurons suggesting morphine could directly affect a subset of these neurons (Gurwell et al., 2001; Bruce-Keller et al., 2008). Thus, we postulate that Tat plus morphine can directly affect synaptodendritic injury, in addition to the concept that MOR-expressing glia principally drive bystander neuronal injury (Gurwell et al., 2001; El-Hage et al., 2005; Zou et al., 2011). Morphine may potentially increase excitation through MOR-dependent $[Ca^{2+}]_i$ increases via G$\beta\gamma$-subunit-dependent phospholipase C activation (Mathews et al., 2008). The resultant IP_3-dependent increases in $[Ca^{2+}]_i$ potentiate Ca^{2+}-induced Ca^{2+} release via ryanodine receptors (Fig. 8). Without additional study, however, it is difficult to know the extent to which the excitotoxic effects are secondary to direct actions in astrocytes and/or microglia, or network effects. Prior studies implicating marked glial involvement have been largely limited to assessing neuronal death (Zou et al., 2011). Cell death aside, our data suggest that Tat ± morphine can directly compromise the structural and functional integrity of striatal neurons.

The primary rewarding effects of opioids are largely mediated by MOR in the ventral tegmental area (VTA; Wise, 1989), the activation of which leads to increased firing of dopaminergic neu-

rons (Johnson and North, 1992). This opioid-mediated effect was later shown to additionally require activation of VTA NMDA and AMPA receptors (Harris et al., 2004; Jalabert et al., 2011). Increased firing of dopaminergic neurons leads to increased dopamine release in limbic forebrain structures including the ventral striatum, where the NR2B subunit of the NMDAR has been shown to regulate the development of a morphine conditioned place preference (Kao et al., 2011). The conditioned place preference assay is used to model the primary rewarding, motivational, and/or conditioning effects of commonly abused substances (Bardo and Bevins, 2000). Intriguingly, intracerebral ventricular infusion of subunit-specific blocking antibodies revealed that NR2B, but not NR1 or NR2A subunits mediated acquisition of a morphine place preference (Narita et al., 2000). In contrast, microinjection of AMPA/kainate receptor antagonists into the ventral striatum blocked the expression, but not acquisition of a morphine conditioned place preference (Layer et al., 1993). Similarly, ventral striatal AMPA/kainate receptor antagonists blocked the cue- and drug-provoked reinstatement of previously extinguished heroin-seeking behavior (LaLumiere and Kalivas, 2008), and NMDAR blockers modestly reduced subjective responses to heroin in humans. When considering these studies together with the present findings, the possibility emerges that opiate-abusing individuals with HAND/neuroAIDS may be more prone to rate opioid experiences positively and potentially to crave more drug.

References

Aksenov MY, Aksenova MV, Mactutus CF, Booze RM (2012) D1/NMDA receptors and concurrent methamphetamine + HIV-1 Tat neurotoxicity. J Neuroimmune Pharmacol 7:599–608. CrossRef Medline

Al-Shaikhaly MH, Nedergaard J, Cannon B (1979) Sodium-induced calcium release from mitochondria in brown adipose tissue. Proc Natl Acad Sci U S A 76:2350–2353. CrossRef Medline

Anthony IC, Arango JC, Stephens B, Simmonds P, Bell JE (2008) The effects of illicit drugs on the HIV infected brain. Front Biosci 13:1294–1307. CrossRef Medline

Bardo MT, Bevins RA (2000) Conditioned place preference: what does it add to our preclinical understanding of drug reward? Psychopharmacology (Berl) 153:31–43. CrossRef Medline

Bell JE, Brettle RP, Chiswick A, Simmonds P (1998) HIV encephalitis, proviral load and dementia in drug users and homosexuals with AIDS: effect of neocortical involvement. Brain 121:2043–2052. CrossRef Medline

Berridge MJ (1987) Inositol trisphosphate and diacylglycerol: two interacting second messengers. Annu Rev Biochem 56:159–193. CrossRef Medline

Bertrand SJ, Aksenova MV, Mactutus CF, Booze RM (2013) HIV-1 Tat protein variants: critical role for the cysteine region in synaptodendritic injury. Exp Neurol 248:228–235. CrossRef Medline

Bertrand SJ, Mactutus CF, Aksenova MV, Espensen-Sturges TD, Booze RM (2014) Synaptodendritic recovery following HIV Tat exposure: neurorestoration by phytoestrogens. J Neurochem 128:140–151. CrossRef Medline

Bindokas VP, Miller RJ (1995) Excitotoxic degeneration is initiated at nonrandom sites in cultured rat cerebellar neurons. J Neurosci 15:6999–7011. Medline

Bruce-Keller AJ, Turchan-Cholewo J, Smart EJ, Geurin T, Chauhan A, Reid R, Xu R, Nath A, Knapp PE, Hauser KF (2008) Morphine causes rapid increases in glial activation and neuronal injury in the striatum of inducible HIV-1 Tat transgenic mice. Glia 56:1414–1427. CrossRef Medline

Burbassi S, Sengupta R, Meucci O (2010) Alterations of CXCR4 function in mu-opioid receptor-deficient glia. Eur J Neurosci 32:1278–1288. CrossRef Medline

Byrd DA, Fellows RP, Morgello S, Franklin D, Heaton RK, Deutsch R, Atkinson JH, Clifford DB, Collier AC, Marra CM, Gelman B, McCutchan JA, Duarte NA, Simpson DM, McArthur J, Grant I (2011) Neurocognitive impact of substance use in HIV infection. J Acquir Immune Defic Syndr 58:154–162. CrossRef Medline

Carey AN, Sypek EI, Singh HD, Kaufman MJ, McLaughlin JP (2012) Expression of HIV-Tat protein is associated with learning and memory deficits in the mouse. Behav Brain Res 229:48–56. CrossRef Medline

Chefer VI, Denoroy L, Zapata A, Shippenberg TS (2009) Mu opioid receptor modulation of somatodendritic dopamine overflow: GABAergic and glutamatergic mechanisms. Eur J Neurosci 30:272–278. CrossRef Medline

Cheng J, Nath A, Knudsen B, Hochman S, Geiger JD, Ma M, Magnuson DS (1998) Neuronal excitatory properties of human immunodeficiency virus type 1 Tat protein. Neuroscience 82:97–106. CrossRef Medline

Dever SM, Costin BN, Xu R, El-Hage N, Balinang J, Samoshkin A, O'Brien MA, McRae M, Diatchenko L, Knapp PE, Hauser KF (2014) Differential expression of the alternatively spliced *OPRM1* isoform μ-opioid receptor-1K in HIV-infected individuals. AIDS 28:19–30. CrossRef Medline

Dingledine R, Borges K, Bowie D, Traynelis SF (1999) The glutamate receptor ion channels. Pharmacol Rev 51:7–61. Medline

El-Hage N, Gurwell JA, Singh IN, Knapp PE, Nath A, Hauser KF (2005) Synergistic increases in intracellular Ca^{2+}, and the release of MCP-1, RANTES, and IL-6 by astrocytes treated with opiates and HIV-1 Tat. Glia 50:91–106. CrossRef Medline

El-Hage N, Bruce-Keller AJ, Yakovleva T, Bazov I, Bakalkin G, Knapp PE, Hauser KF (2008) Morphine exacerbates HIV-1 Tat-induced cytokine production in astrocytes through convergent effects on $[Ca^{2+}]_i$, NF-κB trafficking and transcription. PLoS One 3:e4093. CrossRef Medline

Eugenin EA, King JE, Hazleton JE, Major EO, Bennett MV, Zukin RS, Berman JW (2011) Differences in NMDA receptor expression during human development determine the response of neurons to HIV-tat-mediated neurotoxicity. Neurotox Res 19:138–148. CrossRef Medline

Fitting S, Xu R, Bull C, Buch SK, El-Hage N, Nath A, Knapp PE, Hauser KF (2010) Interactive comorbidity between opioid drug abuse and HIV-1 Tat: chronic exposure augments spine loss and sublethal dendritic pathology in striatal neurons. Am J Pathol 177:1397–1410. CrossRef Medline

Fitting S, Ignatowska-Jankowska BM, Bull C, Skoff RP, Lichtman AH, Wise LE, Fox MA, Su J, Medina AE, Krahe TE, Knapp PE, Guido W, Hauser KF (2013) Synaptic dysfunction in the hippocampus accompanies learning and memory deficits in human immunodeficiency virus type-1 Tat transgenic mice. Biol Psychiatry 73:443–453. CrossRef Medline

Greenhouse SW, Geisser S (1959) On methods in the analysis of profile data. Psychometrika 24:95–112. CrossRef

Greenwood SM, Connolly CN (2007) Dendritic and mitochondrial changes during glutamate excitotoxicity. Neuropharmacology 53:891–898. CrossRef Medline

Gris P, Gauthier J, Cheng P, Gibson DG, Gris D, Laur O, Pierson J, Wentworth S, Nackley AG, Maixner W, Diatchenko L (2010) A novel alternatively spliced isoform of the mu-opioid receptor: functional antagonism. Mol Pain 6:33. CrossRef Medline

Grynkiewicz G, Poenie M, Tsien RY (1985) A new generation of Ca^{2+} indicators with greatly improved fluorescence properties. J Biol Chem 260:3440–3450. Medline

Gurwell JA, Nath A, Sun Q, Zhang J, Martin KM, Chen Y, Hauser KF (2001) Synergistic neurotoxicity of opioids and human immunodeficiency virus-1 Tat protein in striatal neurons in vitro. Neuroscience 102:555–563. CrossRef Medline

Hahn YK, Podhaizer EM, Farris SP, Miles MF, Hauser KF, Knapp PE (2014) Effects of chronic HIV-1 Tat exposure in the CNS: heightened vulnerability of males versus females to changes in cell numbers, synaptic integrity, and behavior. Brain Struct Funct. Advance online publication. Retrieved December 2013. CrossRef Medline

Hardingham GE (2009) Coupling of the NMDA receptor to neuroprotective and neurodestructive events. Biochem Soc Trans 37:1147–1160. CrossRef Medline

Harris GC, Wimmer M, Byrne R, Aston-Jones G (2004) Glutamate-associated plasticity in the ventral tegmental area is necessary for conditioning environmental stimuli with morphine. Neuroscience 129:841–847. CrossRef Medline

Haughey NJ, Holden CP, Nath A, Geiger JD (1999) Involvement of inositol 1,4,5-trisphosphate-regulated stores of intracellular calcium in calcium dysregulation and neuron cell death caused by HIV-1 protein Tat. J Neurochem 73:1363–1374. CrossRef Medline

Haughey NJ, Nath A, Mattson MP, Slevin JT, Geiger JD (2001) HIV-1 Tat

through phosphorylation of NMDA receptors potentiates glutamate excitotoxicity. J Neurochem 78:457–467. CrossRef Medline

Hauser KF, Stiene-Martin A, Mattson MP, Elde RP, Ryan SE, Godleske CC (1996) μ-Opioid receptor-induced Ca^{2+} mobilization and astroglial development: morphine inhibits DNA synthesis and stimulates cellular hypertrophy through a Ca^{2+}-dependent mechanism. Brain Res 720:191–203. CrossRef Medline

Heaton RK, Franklin DR, Ellis RJ, McCutchan JA, Letendre SL, Leblanc S, Corkran SH, Duarte NA, Clifford DB, Woods SP, Collier AC, Marra CM, Morgello S, Mindt MR, Taylor MJ, Marcotte TD, Atkinson JH, Wolfson T, Gelman BB, McArthur JC, et al. (2011) HIV-associated neurocognitive disorders before and during the era of combination antiretroviral therapy: differences in rates, nature, and predictors. J Neurovirol 17:3–16. CrossRef Medline

Jalabert M, Bourdy R, Courtin J, Veinante P, Manzoni OJ, Barrot M, Georges F (2011) Neuronal circuits underlying acute morphine action on dopamine neurons. Proc Natl Acad Sci U S A 108:16446–16450. CrossRef Medline

Johnson SW, North RA (1992) Opioids excite dopamine neurons by hyperpolarization of local interneurons. J Neurosci 12:483–488. Medline

Kao JH, Huang EY, Tao PL (2011) NR2B subunit of NMDA receptor at nucleus accumbens is involved in morphine rewarding effect by siRNA study. Drug Alcohol Depend 118:366–374. CrossRef Medline

Kiedrowski L (1999) N-methyl-D-aspartate excitotoxicity: relationships among plasma membrane potential, Na^+/Ca^{2+} exchange, mitochondrial Ca^{2+} overload, and cytoplasmic concentrations of Ca^{2+}, H^+, and K^+. Mol Pharmacol 56:619–632. CrossRef Medline

Kreitzer AC (2009) Physiology and pharmacology of striatal neurons. Annu Rev Neurosci 32:127–147. CrossRef Medline

Krisher RL, Prather RS (2012) A role for the Warburg effect in preimplantation embryo development: metabolic modification to support rapid cell proliferation. Mol Reprod Dev 79:311–320. CrossRef Medline

Kruman II, Nath A, Mattson MP (1998) HIV-1 protein Tat induces apoptosis of hippocampal neurons by a mechanism involving caspase activation, calcium overload, and oxidative stress. Exp Neurol 154:276–288. CrossRef Medline

LaLumiere RT, Kalivas PW (2008) Glutamate release in the nucleus accumbens core is necessary for heroin seeking. J Neurosci 28:3170–3177. CrossRef Medline

Laurent V, Leung B, Maidment N, Balleine BW (2012) μ- and δ-Opioid-related processes in the accumbens core and shell differentially mediate the influence of reward-guided and stimulus-guided decisions on choice. J Neurosci 32:1875–1883. CrossRef Medline

Layer RT, Uretsky NJ, Wallace LJ (1993) Effects of the AMPA/kainate receptor antagonist DNQX in the nucleus accumbens on drug-induced conditioned place preference. Brain Res 617:267–273. CrossRef Medline

Liao D, Lin H, Law PY, Loh HH (2005) Mu-opioid receptors modulate the stability of dendritic spines. Proc Natl Acad Sci U S A 102:1725–1730. CrossRef Medline

Liao D, Grigoriants OO, Wang W, Wiens K, Loh HH, Law PY (2007) Distinct effects of individual opioids on the morphology of spines depend upon the internalization of mu opioid receptors. Mol Cell Neurosci 35:456–469. CrossRef Medline

Li W, Huang Y, Reid R, Steiner J, Malpica-Llanos T, Darden TA, Shankar SK, Mahadevan A, Satishchandra P, Nath A (2008) NMDA receptor activation by HIV-Tat protein is clade dependent. J Neurosci 28:12190–12198. CrossRef Medline

Liu Y, Wong TP, Aarts M, Rooyakkers A, Liu L, Lai TW, Wu DC, Lu J, Tymianski M, Craig AM, Wang YT (2007) NMDA receptor subunits have differential roles in mediating excitotoxic neuronal death both in vitro and in vivo. J Neurosci 27:2846–2857. CrossRef Medline

Longordo F, Feligioni M, Chiaramonte G, Sbaffi PF, Raiteri M, Pittaluga A (2006) The human immunodeficiency virus-1 protein transactivator of transcription upregulates N-methyl-D-aspartate receptor function by acting at metabotropic glutamate receptor 1 receptors coexisting on human and rat brain noradrenergic neurones. J Pharmacol Exp Ther 317:1097–1105. CrossRef Medline

Lui PW, Suen KC, Chan YS, Yung WH, Yung KK (2003) Striatal neurons but not nigral dopaminergic neurons in neonatal primary cell culture express endogenous functional *N*-methyl-D-aspartate receptors. Mol Brain Res 120:9–21. CrossRef Medline

MacMillan D, Chalmers S, Muir TC, McCarron JG (2005) IP_3-mediated Ca^{2+} increases do not involve the ryanodine receptor, but ryanodine receptor antagonists reduce IP_3-mediated Ca^{2+} increases in guinea-pig colonic smooth muscle cells. J Physiol 569:533–544. CrossRef Medline

Magnuson DS, Knudsen BE, Geiger JD, Brownstone RM, Nath A (1995) Human immunodeficiency virus type 1 tat activates non-*N*-methyl-D-aspartate excitatory amino acid receptors and causes neurotoxicity. Ann Neurol 37:373–380. CrossRef Medline

Marin P, Quignard JF, Lafon-Cazal M, Bockaert J (1993) Non-classical glutamate receptors, blocked by both NMDA and non-NMDA antagonists, stimulate nitric oxide production in neurons. Neuropharmacology 32:29–36. CrossRef Medline

Martin M, Matifas A, Maldonado R, Kieffer BL (2003) Acute antinociceptive responses in single and combinatorial opioid receptor knockout mice: distinct mu, delta and kappa tones. Eur J Neurosci 17:701–708. CrossRef Medline

Masliah E, Heaton RK, Marcotte TD, Ellis RJ, Wiley CA, Mallory M, Achim CL, McCutchan JA, Nelson JA, Atkinson JH, Grant I (1997) Dendritic injury is a pathological substrate for human immunodeficiency virus-related cognitive disorders: HNRC Group. The HIV Neurobehavioral Research Center. Ann Neurol 42:963–972. CrossRef Medline

Mathews JL, Smrcka AV, Bidlack JM (2008) A novel Gβγ-subunit inhibitor selectively modulates mu-opioid-dependent antinociception and attenuates acute morphine-induced antinociceptive tolerance and dependence. J Neurosci 28:12183–12189. CrossRef Medline

Matthes HW, Maldonado R, Simonin F, Valverde O, Slowe S, Kitchen I, Befort K, Dierich A, Le Meur M, Dollé P, Tzavara E, Hanoune J, Roques BP, Kieffer BL (1996) Loss of morphine-induced analgesia, reward effect and withdrawal symptoms in mice lacking the μ-opioid-receptor gene. Nature 383:819–823. CrossRef Medline

Mattson MP, Haughey NJ, Nath A (2005) Cell death in HIV dementia. Cell Death Differ 12:893–904. CrossRef Medline

Mattson MP, Gleichmann M, Cheng A (2008) Mitochondria in neuroplasticity and neurological disorders. Neuron 60:748–766. CrossRef Medline

McBain CJ, Mayer ML (1994) N-methyl-D-aspartic acid receptor structure and function. Physiol Rev 74:723–760. Medline

Menegon A, Leoni C, Benfenati F, Valtorta F (1997) Tat protein from HIV-1 activates MAP kinase in granular neurons and glial cells from rat cerebellum. Biochem Biophys Res Commun 238:800–805. CrossRef Medline

Midde NM, Huang X, Gomez AM, Booze RM, Zhan CG, Zhu J (2013) Mutation of tyrosine 470 of human dopamine transporter is critical for HIV-1 Tat-induced inhibition of dopamine transport and transporter conformational transitions. J Neuroimmune Pharmacol 8:975–987. CrossRef Medline

Narita M, Aoki T, Suzuki T (2000) Molecular evidence for the involvement of NR2B subunit containing *N*-methyl-D-aspartate receptors in the development of morphine-induced place preference. Neuroscience 101:601–606. CrossRef Medline

Nath A, Psooy K, Martin C, Knudsen B, Magnuson DS, Haughey N, Geiger JD (1996) Identification of a human immunodeficiency virus type 1 Tat epitope that is neuroexcitatory and neurotoxic. J Virol 70:1475–1480. Medline

Nath A, Booze RM, Hauser KF, Mactutus CF, Bell JE, Maragos WF, Berger JR (1999) Critical questions for neuroscientists in interactions of drugs of abuse and HIV infection. NeuroAIDS 2:1–12.

Nicholls DG, Johnson-Cadwell L, Vesce S, Jekabsons M, Yadava N (2007) Bioenergetics of mitochondria in cultured neurons and their role in glutamate excitotoxicity. J Neurosci Res 85:3206–3212. CrossRef Medline

Nishizuka Y (1988) The molecular heterogeneity of protein kinase C and its implications for cellular regulation. Nature 334:661–665. CrossRef Medline

Norman JP, Perry SW, Kasischke KA, Volsky DJ, Gelbard HA (2007) HIV-1 trans activator of transcription protein elicits mitochondrial hyperpolarization and respiratory deficit, with dysregulation of complex IV and nicotinamide adenine dinucleotide homeostasis in cortical neurons. J Immunol 178:869–876. CrossRef Medline

Norman JP, Perry SW, Reynolds HM, Kiebala M, De Mesy Bentley KL, Trejo M, Volsky DJ, Maggirwar SB, Dewhurst S, Masliah E, Gelbard HA (2008) HIV-1 Tat activates neuronal ryanodine receptors with rapid induction of the unfolded protein response and mitochondrial hyperpolarization. PLoS One 3:e3731. CrossRef Medline

Olney JW, Price MT, Samson L, Labruyere J (1986) The role of specific ions in glutamate neurotoxicity. Neurosci Lett 65:65–71. CrossRef Medline

Paris JJ, Singh HD, Ganno ML, Jackson P, McLaughlin JP (2014) Anxiety-like behavior of mice produced by conditional central expression of the HIV-1 regulatory protein, Tat. Psychopharmacology (Berl) 231:2349–2360. CrossRef Medline

Pepponi R, Ferrante A, Ferretti R, Martire A, Popoli P (2009) Region-specific neuroprotective effect of ZM 241385 towards glutamate uptake inhibition in cultured neurons. Eur J Pharmacol 617:28–32. CrossRef Medline

Pérez A, Probert AW, Wang KK, Sharmeen L (2001) Evaluation of HIV-1 Tat induced neurotoxicity in rat cortical cell culture. J Neurovirol 7:1–10. CrossRef Medline

Perry SW, Norman JP, Gelbard HA (2005) Adjunctive therapies for HIV-1 associated neurologic disease. Neurotox Res 8:161–166. CrossRef Medline

Perry SW, Barbieri J, Tong N, Polesskaya O, Pudasaini S, Stout A, Lu R, Kiebala M, Maggirwar SB, Gelbard HA (2010) Human immunodeficiency virus-1 Tat activates calpain proteases via the ryanodine receptor to enhance surface dopamine transporter levels and increase transporter-specific uptake and V_{max}. J Neurosci 30:14153–14164. CrossRef Medline

Perry SW, Norman JP, Barbieri J, Brown EB, Gelbard HA (2011) Mitochondrial membrane potential probes and the proton gradient: a practical usage guide. Biotechniques 50:98–115. CrossRef Medline

Podhaizer EM, Zou S, Fitting S, Samano KL, El-Hage N, Knapp PE, Hauser KF (2012) Morphine and gp120 toxic interactions in striatal neurons are dependent on HIV-1 strain. J Neuroimmune Pharmacol 7:877–891. CrossRef Medline

Rothman SM (1985) The neurotoxicity of excitatory amino acids is produced by passive chloride influx. J Neurosci 5:1483–1489. Medline

Ruiz C, Casarejos MJ, Rubio I, Gines S, Puigdellivol M, Alberch J, Mena MA, de Yebenes JG (2012) The dopaminergic stabilizer, (-)-OSU6162, rescues striatal neurons with normal and expanded polyglutamine chains in huntingtin protein from exposure to free radicals and mitochondrial toxins. Brain Res 1459:100–112. CrossRef Medline

Singh IN, Goody RJ, Dean C, Ahmad NM, Lutz SE, Knapp PE, Nath A, Hauser KF (2004) Apoptotic death of striatal neurons induced by human immunodeficiency virus-1 Tat and gp120: differential involvement of caspase-3 and endonuclease G. J Neurovirol 10:141–151. CrossRef Medline

Stefani A, Chen Q, Flores-Hernandez J, Jiao Y, Reiner A, Surmeier DJ (1998) Physiological and molecular properties of AMPA/kainate receptors expressed by striatal medium spiny neurons. Dev Neurosci 20:242–252. CrossRef Medline

Suzuki M, El-Hage N, Zou S, Hahn YK, Sorrell ME, Sturgill JL, Conrad DH, Knapp PE, Hauser KF (2011) Fractalkine/CX3CL1 protects striatal neurons from synergistic morphine and HIV-1 Tat-induced dendritic losses and death. Mol Neurodegener 6:78. CrossRef Medline

Tichelaar W, Safferling M, Keinänen K, Stark H, Madden DR (2004) The three-dimensional structure of an ionotropic glutamate receptor reveals a dimer-of-dimers assembly. J Mol Biol 344:435–442. CrossRef Medline

Vander Jagt TA, Connor JA, Shuttleworth CW (2008) Localized loss of Ca^{2+} homeostasis in neuronal dendrites is a downstream consequence of metabolic compromise during extended NMDA exposures. J Neurosci 28:5029–5039. CrossRef Medline

Wang X, Loram LC, Ramos K, de Jesus AJ, Thomas J, Cheng K, Reddy A, Somogyi AA, Hutchinson MR, Watkins LR, Yin H (2012) Morphine activates neuroinflammation in a manner parallel to endotoxin. Proc Natl Acad Sci U S A 109:6325–6330. CrossRef Medline

Wise RA (1989) Opiate reward: sites and substrates. Neurosci Biobehav Rev 13:129–133. CrossRef Medline

Wolf JA, Stys PK, Lusardi T, Meaney D, Smith DH (2001) Traumatic axonal injury induces calcium influx modulated by tetrodotoxin-sensitive sodium channels. J Neurosci 21:1923–1930. Medline

Xin WK, Kwan CL, Zhao XH, Xu J, Ellen RP, McCulloch CA, Yu XM (2005) A functional interaction of sodium and calcium in the regulation of NMDA receptor activity by remote NMDA receptors. J Neurosci 25:139–148. CrossRef Medline

Yu SP, Choi DW (1997) Na^{+}-Ca^{2+} exchange currents in cortical neurons: concomitant forward and reverse operation and effect of glutamate. Eur J Neurosci 9:1273–1281. CrossRef Medline

Yu XM (2006) The role of intracellular sodium in the regulation of NMDA-receptor-mediated channel activity and toxicity. Mol Neurobiol 33:63–80. CrossRef Medline

Yu XM, Salter MW (1998) Gain control of NMDA-receptor currents by intracellular sodium. Nature 396:469–474. CrossRef Medline

Zhao F, Li P, Chen SR, Louis CF, Fruen BR (2001) Dantrolene inhibition of ryanodine receptor Ca^{2+} release channels.: molecular mechanism and isoform selectivity. J Biol Chem 276:13810–13816. CrossRef Medline

Zhu J, Mactutus CF, Wallace DR, Booze RM (2009) HIV-1 Tat protein-induced rapid and reversible decrease in [^{3}H]dopamine uptake: dissociation of [^{3}H]dopamine uptake and [^{3}H]2β-carbomethoxy-3-β-(4-fluorophenyl) tropane (WIN 35,428) binding in rat striatal synaptosomes. J Pharmacol Exp Ther 329:1071–1083. CrossRef Medline

Zou S, Fitting S, Hahn YK, Welch SP, El-Hage N, Hauser KF, Knapp PE (2011) Morphine potentiates neurodegenerative effects of HIV-1 Tat through actions at μ-opioid receptor-expressing glia. Brain 134:3616–3631. CrossRef Medline